Oscillatory Mechanisms of Preparing for Visual Distraction

de Vries, Ingmar E.J.; Savran, Ece; van Driel, Joram; Olivers, Christian N.L.

published in
Journal of cognitive neuroscience
2019

DOI (link to publisher)
10.1162/jocn_a_01460

document version
Publisher's PDF, also known as Version of record

Oscillatory Mechanisms of Preparing for Visual Distraction

Ingmar E. J. de Vries, Ece Savran, Joram van Driel, and Christian N. L. Olivers

Abstract

■ Evidence shows that observers preactivate a target representation in preparation of a visual selection task. In this study, we addressed the question if and how preparing to ignore an anticipated distractor differs from preparing for an anticipated target. We measured EEG while participants memorized a laterally presented color, which was cued to be either a target or a distractor in two subsequent visual search tasks. Decoding the location of items in the search display from EOG channels revealed that, initially, the anticipated distractor attracted attention and could only be ignored later during the trial. This suggests that distractors could not be suppressed in advance but were represented in an active, attention-guiding format. Consistent with this, lateralized posterior alpha power did not dissociate between target and distractor templates during the delay periods, suggesting similar encoding and maintenance. However, distractor preparation did lead to relatively enhanced nonlateralized posterior alpha power, which appeared to gate sensory processing at search display onset to prevent attentional capture in general. Finally, anticipating distractors also led to enhanced midfrontal theta power during the delay period, a signal that was predictive of how strongly both target and distractor were represented in the search display. Together, our results speak against a distractor-specific advance inhibitory template, thus contrary to the preactivation of specific target templates. Rather, we demonstrate a general selection suppression mechanism, which serves to prevent initial involuntary capture by anticipated distracting input. ■

INTRODUCTION

Selecting relevant, while ignoring irrelevant, visual information from our environment is an essential element of everyday life. To aid selection, we typically preactivate a task-relevant target representation, also termed the "attentional template," that helps guide our attention toward matching visual input (Desimone & Duncan, 1995; Duncan & Humphreys, 1989), and that governing models assume to be activated in visual working memory (Itti & Koch, 2001; Wolfe, 1994; Bundesen, 1990). Consistent with this, accounts inspired by neuroimaging data propose that primary visual areas maintain sensory information in service of our current perceptual goals (Gazzaley & Nobre, 2012; Harrison & Tong, 2009; Serences, Ester, Vogel, & Awh, 2009; Postle, 2006; Pasternak & Greenlee, 2005). These representations may undergo a flexible functional transformation toward a task-specific representational state, to optimize target detection (Gayet et al., 2017; Myers, Rohenkohl, et al., 2015; Olivers & Eimer, 2011; Olivers, Peters, Houtkamp, & Roelfsema, 2011) and perception–action mapping (Myers, Stokes, & Nobre, 2017).

However, in some situations, one is informed on which information will be irrelevant, rather than relevant. How do observers prepare for ignoring anticipated distractor information? And how does this mechanistically differ from preactivating an anticipated target representation? One option is what we will refer to as the "advance inhibitory template" hypothesis, which postulates that anticipated distractors can be ignored by preemptively suppressing the distractor representation before exposure (i.e., a so-called template for rejection; Gaspelin & Luck, 2018b; Woodman & Luck, 2007). Whereas stimuli matching the target template in memory are more likely to capture attention, stimuli matching the distractor template in memory would then be less likely to capture attention, resulting in a behavioral benefit relative to unexpected distractors. A second option is what we will refer to as the "reactive reorienting" hypothesis, which states that an anticipated distractor is in principle processed in the same way as an anticipated target, until the actual distractor is encountered, after which observers orient away from it. This account predicts that the distractor is actually initially selected before observers can reorient toward the actual target. Some have argued that observers may strategically do so (referred to as "seek and destroy" by Moher & Egeth, 2012), but there is also evidence showing that anything actively held in working memory will automatically capture attention, even when detrimental to performance (Olivers, Meijer, & Theeuwes, 2006; Soto, Heinke, Humphreys, & Blanco, 2005)—analogous to the paradoxical process of trying "to avoid a white bear" (Tsal & Makovski, 2006; Wegner, Schneider, Carter, & White, 1987). A third option is what

Vrije Universiteit Amsterdam

Journal of Cognitive Neuroscience 31:12, pp. 1873–1894
https://doi.org/10.1162/jocn_a_01460

we will refer to as the "general selection suppression" hypothesis (Noonan, Crittenden, Jensen, & Stokes, 2018; Reeder, Olivers, Hanke, & Pollmann, 2018), which may in fact be a strategy to deal with the involuntary capture by anticipated distractors. This account predicts that the early involuntary phase of selection is suppressed, after which a more controlled voluntary selection of the target can be made.

Despite extensive research, the crucial question how one mechanistically prepares for an anticipated distractor remains unanswered. In this study, we addressed this issue by measuring EEG while participants memorized a color needed for two subsequent visual search tasks, each preceded by a delay period (see Figure 1 for illustration). Importantly, an auditory cue at onset of each delay period informed whether the template would serve as a target or a distractor on the subsequent search task. We focused on oscillatory measures to assess if target and distractor templates differ in their neural implementation. If so, we should also be able to observe a change in status for a given template held in working memory when it first signifies a target and then a distractor, or vice versa. To this end, we presented two search tasks per trial, and the status of the template either repeated or switched from the first to the second search task.

One candidate neural mechanism that may distinguish between target and distractor templates is oscillatory

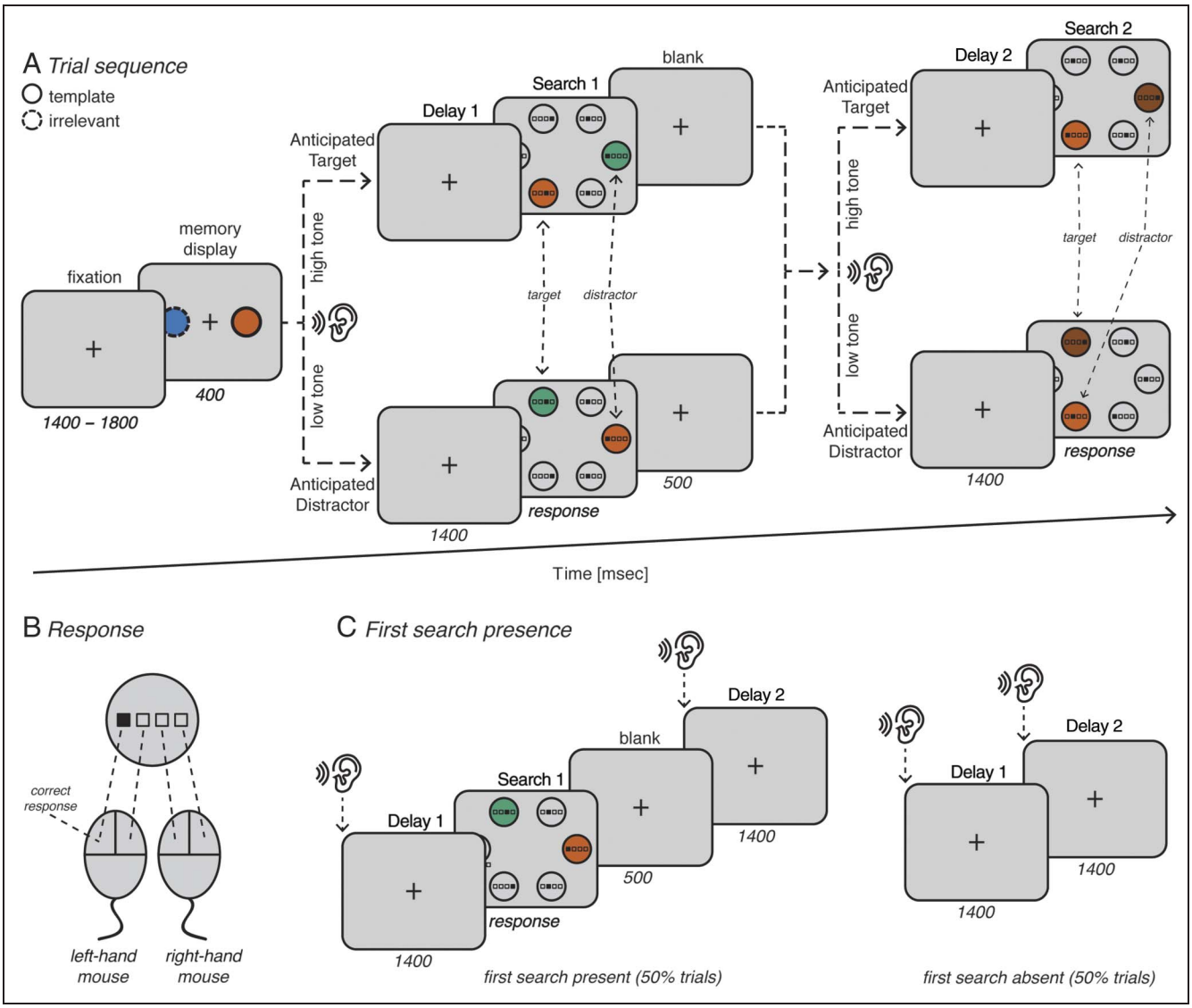

Figure 1. Task design. (A) Trial sequence. Participants were given one color template to remember (from a display of two), after which they performed two consecutive search tasks. The template (here indicated by a full outline) was always presented left or right from fixation and indicated which color to anticipate. The onsets of Delay 1 and Delay 2 were accompanied by a tone, informing the participant on whether, in the subsequent search task, the anticipated color would serve as the target or as the distractor. For illustrative purposes, object sizes and colors differ somewhat from the real experiment. (B) Participants held a mouse in each hand and responded by pressing the mouse button belonging to the filled square (of four small squares presented inside the selected color). (C) As we were interested in the switching template status during the second delay, we omitted the first search display in a random 50% of trials, to prevent interference with the EEG signals related to the second delay period. Here, the screen remained blank (with a fixation cross), and the start of the second delay period was marked by the second auditory cue.

activity in the alpha frequency range as measured from electrodes above visual areas. Spatiotopically selective posterior alpha power increases in preparation of anticipated distraction at an expected spatial location (Händel, Haarmeier, & Jensen, 2011; Rihs, Michel, & Thut, 2007; Worden, Foxe, Wang, & Simpson, 2000). Furthermore, overall posterior alpha power generally increases during working memory maintenance when distractors are expected and working memory should be protected from interference (Payne, Guillory, & Sekuler, 2013; Bonnefond & Jensen, 2012; although see Schroeder, Ball, & Busch, 2018). Posterior alpha enhancement is generally thought of as an inhibitory process that prevents selection and processing of irrelevant sensory information (Zumer, Scheeringa, Schoffelen, Norris, & Jensen, 2014; Foxe & Snyder, 2011; Jensen & Mazaheri, 2010; Sauseng et al., 2009; Klimesch, Sauseng, & Hanslmayr, 2007). Crucial for the matter at hand, posterior alpha enhancement not only shields perceptual information from interfering with working memory, it also operates inversely by shielding irrelevant memories from interfering with the current task (de Vries, van Driel, Karacaoglu, & Olivers, 2018; Waldhauser, Johansson, & Hanslmayr, 2012). Specifically, when a working memory becomes irrelevant, alpha is selectively enhanced for the spatial location at which it was originally presented (Schneider, Göddertz, Haase, Hickey, & Wascher, 2019; de Vries et al., 2018). This effect emerges a considerable time after memory encoding, despite spatial location being task irrelevant, thus revealing the suppression of memory item-specific sensory processing in early visual areas. Therefore, under the advance inhibitory template hypothesis, one would expect advance posterior alpha enhancement selectively for the retinotopic location at which this item was processed, as to suppress the anticipated distractor information in memory. In contrast, under the reactive orienting hypothesis, one would expect to observe the same posterior alpha modulation for anticipated targets and anticipated distractors, at least during preparation and initial selection. Last, under the general selection suppression hypothesis, one would instead expect to observe overall posterior alpha enhancement for the anticipated distractor at search onset, reflecting the momentary suppression of any visual selection from the search display to prevent inadvertent attentional capture.

Furthermore, because frontal cortex has been implicated in the executive control of both anticipatory and reactive distractor suppression (Geng, 2014), we expected involvement of frontal cortical regions here as well. Low-frequency oscillations above frontal regions have long been implicated in cognitive control mechanisms in general (Helfrich, Huang, Wilson, & Knight, 2017; Cavanagh & Frank, 2014) and in working memory operations specifically (Johnson et al., 2017; Sauseng, Griesmayr, Freunberger, & Klimesch, 2010; Onton, Delorme, & Makeig, 2005; Jensen & Tesche, 2002). We previously observed frontal delta (2–4 Hz) oscillations to flexibly control the priority of specific working memory representations, depending on moment-by-moment perceptual goals (de Vries, van Driel, & Olivers, 2019; de Vries et al., 2018). Therefore, we expected frontal delta power to also play a key role in controlling the states of target and distractor templates as well as the switching thereof.

METHODS

Participants

We planned a minimum of 20 healthy human participants for our final analyses but collected data from 26 to accommodate the anticipated usual removal of a few participants because of poor performance, noisy EEG data, or other technical issues. In total, four participants were removed—three because they made too many horizontal eye movements during the memory display (at least 18% of trials) and one because the first part of the experiment was accidentally not saved—thus leaving 22 participants (14 women, 24 ± 3 years old) for all analyses. Participants had normal or corrected-to-normal vision and participated for course credit or monetary compensation. All procedures used were conducted in accordance with the Declaration of Helsinki and were positively reviewed by the faculty's Scientific and Ethical Review Board (VCWE-2016-215). Written informed consent was obtained.

Task Design

Figure 1A illustrates the trial procedure. Each trial started with a fixation cross (1400–1800 msec, randomly jittered), subsequently followed by a memory display (400 msec), the first delay period (1400 msec; which started with a 50-msec auditory cue), the first search display (until response), a blank recovery period (500 msec), the second delay period (1400 msec; which also started with a 50-msec auditory cue), and, finally, the second search display (until response). The memory display consisted of two colored circles, left and right of fixation, of which participants memorized one and ignored the other (which was solely there for display balancing purposes). The type of outline (dashed or full, counterbalanced across participants) indicated the to-be-remembered color, which served as the template for which color to anticipate. The main factor was the template status—that is, whether the anticipated color indicated the target (Anticipated Target [AT] condition) or the distractor (Anticipated Distractor [AD] condition). The auditory cues at the onsets of Delay 1 and Delay 2 informed observers on this, with a high tone indicating that the color would be the target and a low tone indicating that it would be a distractor. Each search display consisted of four gray circles, plus two colored circles, one of which served as the target whereas the other served as a salient distractor.

In the AT condition, the search target would carry the anticipated color, whereas the remaining, unanticipated color in the display would be the salient distractor. In contrast, in the AD condition, the distractor would carry the anticipated color, and the remaining unanticipated color would then automatically serve as the target. Crucially, because the search displays themselves contained no information as to which colored circle was the target and which was the distractor, participants were required to use the memorized color in combination with the auditory cue to perform the task correctly. Furthermore, the locations of the target and distractor in the search displays were completely independent of each other. After the first search task, the template status could either switch between anticipated target and anticipated distractor or remain the same from one delay period to the next, thus resulting in four possible template combinations: target followed by target template (ATAT), target followed by distractor template (ATAD), distractor followed by target template (ADAT), and distractor followed by distractor template (ADAD).

Each of the six circles in the search display contained four small squares aligned on the horizontal midline, of which one (randomly selected) square was filled (Figure 1B). Upon finding the target, participants responded by pressing one of four mouse buttons (one mouse placed on each armrest) corresponding to the filled square (Figure 1B). Participants focused on a central fixation cross during the intertrial interval, the memory display, and the delay periods. As the memory item was always presented either left or right from fixation, this allowed us to directly relate lateralized EEG patterns to the memory item. To prevent interference from the first search during the second delay, in a random subset of 50% of trials, the first search display and its 500-msec recovery period were omitted, and the screen remained blank (with fixation cross) as the second delay period started with the second auditory cue (Figure 1C). The combination of the omission of the first search display with the auditory cue thus provided the signal to switch to preparing for the second search. Crucially, in our EEG analyses involving the second delay period, we only included these 50% of trials in which the first search display was omitted (Table 1) and that were thus free from any perceptual and response-related activity from the first search task contaminating the second delay period. For the analyses of the second search task itself, we included all trials. Participants performed one practice block followed by 16 experimental blocks, each consisting of a randomly ordered composition of 48 trials, 12 per condition (ATAT, ATAD, ADAT, ADAD), and for each condition, six with and six without the first search task. For the analyses of the first delay period and first search task, we collapsed the ATAT and ATAD conditions and the ADAT and ADAD conditions (because observers could not predict the second search type), thus effectively resulting in two conditions depending on whether the color in memory would be the target (AT) or the distractor (AD) on the first search task. Likewise, for the primary analyses of the second delay period and second search task, we collapsed across the first search template status to assess anticipation of the second task, again resulting in AT (combining ATAT with ADAT) and AD (combining ATAD with ADAD) conditions, but now for the second search. In addition, we assessed switching template status by comparing all four conditions during the second delay period.

Stimuli

Stimuli were created using Opensesame Version 2.9.0 (Mathôt, Schreij, & Theeuwes, 2012, RRID:SCR_002849), a Python-based experiment builder. The experiment was

Table 1. Design and Analysis Plan

Condition Label for Analyses Delay 1 and Search 1	*Condition Label for Analyses Delay 2 and Search 2*	*Included in Analyses Delay 1*	*Included in Analyses Search 1*	*Included in Analyses Delay 2*	*Included in Analyses Search 2*
		First search present			
AT	AT	Yes	Yes	No	Yes
AT	AD	Yes	Yes	No	Yes
AD	AT	Yes	Yes	No	Yes
AD	AD	Yes	Yes	No	Yes
		First search absent			
AT	AT	Yes	No	Yes	Yes
AT	AD	Yes	No	Yes	Yes
AD	AT	Yes	No	Yes	Yes
AD	AD	Yes	No	Yes	Yes

presented on a 22-in. screen (Samsung Syncmaster 2233, 1680 ×1050 pixels at 120 Hz), viewed from a distance of 75 cm. The background was gray (81 Cd/m^2), and the fixation cross was black with line lengths of 0.6°. The two colors in the memory display were presented 1.5° from fixation and had a radius of 0.6° with a black outline of 0.09°. The six circles in the visual search display were presented equidistant from each other and 4° from fixation. Colors were created in DKL color space (Derrington, Krauskopf, & Lennie, 1984) with constant luminance (i.e., 0) and contrast (i.e., 1), but varying in hue (from 12° to 324° in steps of 24°, skipping 108 and 156 because they were subjectively too similar to neighboring colors). This created 12 discrete colors, evenly spaced on an imaginary circle (41.2 ± 4 Cd/m^2). First, for the memory display, the template color was randomly chosen, after which the irrelevant color (presented for sensory balancing) was randomly chosen from the color circle as the opposite color or a color neighboring the opposite color (to prevent too strong similarity). Then, in the search displays, one of the two colors was the anticipated color (whether the target or a distractor), whereas the remaining color present could not be anticipated. This unanticipated color in the display was randomly chosen from the eight colors directly surrounding the anticipated color on the color circle, to increase relative similarity and thereby discourage verbalization and stimulate the use of visual working memory. This strict regulation of color selection resulted in four different colors per trial. The auditory cues were generated by OpenSesame's built-in synthesizer and consisted of 50-msec sine waves at 700 and 4000 Hz for the low and high tones, respectively, presented via Harman Kardon 195 external speakers.

Data Recording and Preprocessing

EEG data were acquired at a sampling rate of 512 Hz using a 64-electrode cap (BioSemi; ActiveTwo system, 10–20 placement; www.biosemi.com) and from two reference electrodes placed on both earlobes. In addition, horizontal and vertical EOGs were recorded from electrodes located 1 cm lateral to the external canthi and from electrodes located 2 cm above and below the right eye, respectively. All offline analyses were performed in MATLAB (2014a, The Mathworks, RRID:SCR_001622). Unless indicated otherwise, preprocessing was done using built-in functions and their default parameter settings as implemented in the EEGLAB toolbox (Delorme & Makeig 2004, RRID:SCR_007292).

First, data were rereferenced to the average of the two reference electrodes. Next, our preprocessing pipeline forked in two EEG data sets; that is, one data set was high-pass filtered at 0.05 Hz, epoched from −2.5 to 9.5 sec surrounding the memory display onset and stored for the last preprocessing step, and the other data set was high-pass filtered at 1.5 Hz to aid data visualization and independent component analysis (ICA) during data cleaning and epoched from −0.5 to 4 sec. Importantly, all choices (trials to reject, channels to interpolate, ICA components to remove) were based on the 1.5-Hz version; the actual cleaning and subsequent analyses were done on the 0.05-Hz version, to prevent filter artifacts influencing multivariate pattern analyses (MVPAs) of electrophysiological data (van Driel, Olivers, & Fahrenfort, 2019). Epochs were baseline-normalized using the whole epoch as baseline for the improvement of ICA (Groppe, Makeig, & Kutas, 2009). Data were visually inspected, and one (n = 6), two (n = 4), or six (n = 1) malfunctioning electrodes were temporarily removed. To specifically detect epochs contaminated by muscle artifacts, we used an adapted version of the automatic trial-rejection procedure as implemented in the Fieldtrip toolbox (Oostenveld, Fries, Maris, & Schoffelen, 2011, RRID:SCR_004849) on the 110- to 140-Hz band-pass filtered data and allowed for individual z score cutoffs. This resulted in a cutoff of 17 ± 5 and a rejection of 6.5% (min–max across participants: 1.6–12.9%) of all trials. After this, we performed ICA on clean trials and electrodes only. We removed an average of 1.6 ± 0.7 ICA components capturing eye movements or blinks (after double-checking this with the EOG signals), or other artifacts that were clearly not brain driven, after which we interpolated the malfunctioning electrodes identified earlier using spherical spline interpolation. Next, we rejected trials on which participants made horizontal eye movements during lateralized memory encoding using the `pop_artstep` function from ERPLAB (Lopez-Calderon & Luck, 2014, RRID:SCR_009574), applied to the 1-Hz high-pass filtered horizontal EOG signal, with a 400-msec window sliding with 10-msec steps, from −50 to 600 msec surrounding memory display onset, and with individual thresholds of 27 ± 5.5. This resulted in a rejection of 5% (min–max across participants: 1.4–11%) of all trials. Last, we identified trials containing power outliers by calculating for each trial the raw power (using wavelet convolution, see subsection Time–Frequency Decomposition), averaged over all frequencies (1–40 Hz), time points, and channels, after which we rejected those trials with a raw power value higher than n standard deviations above the trial median, allowing for an individual n determined by visual inspection. This step specifically identified trials with artifactual spikes or steps, which are likely reflected in all frequency bands and which can have a dramatic impact on further analyses. This resulted in an n of 1 ± 0.8 and a rejection of 1.9% (min–max across participants: 0.1–5.4%) of all trials.

After cleaning the data based on the EEG signals, we also rejected trials with an incorrect response (13%, min–max across participants: 3–25%) and trials with a response faster than 300 msec, slower than 5000 msec, or 3 *SD*s above or below the condition- and search-task-specific mean (2.4%, min–max across participants 1.2–3.0%). After all trial rejection procedures (i.e., based on noisy signals, horizontal eye movements, incorrect responses, and RT), we were left with 73% of all trials

for all EEG analyses (min–max across participants: 57–85%). As a last preprocessing step, we estimated the surface Laplacian using a 10th-order Legendre polynomial and a lambda of 10^{-5} (Perrin, Pernier, Bertrand, & Echallier, 1989). A surface Laplacian is a spatial high-pass filter that accentuates local effects while filtering out distant effects because of volume conduction, thus effectively sharpening the EEG topography (Kayser & Tenke, 2015; Cohen, 2014b). Importantly, we used all trials for analyses of the first delay period, but only those trials in which the first search task was omitted (50%) for analyses of the second delay period, as these trials did not experience interference caused by the first search task (see Table 1).

Location Decoding of Items in the Search Display from EOG

To further elucidate the pattern of behavioral results, we applied an MVPA on the four EOG signals to decode the location of the anticipated color, as well as the remaining, unanticipated color, in the search display. Specifically, we applied a linear discriminant analysis with the four EOG signals as features and the six possible locations in the search display as classes, separately for the anticipated and unanticipated items in each condition. For this MVPA, we used the Amsterdam Decoding and Modeling toolbox (Fahrenfort, van Driel, van Gaal, & Olivers, 2018), an open source, script-based toolbox in MATLAB for backward decoding and forward encoding modeling of EEG/MEG data. Training and testing were done on the same data using a 10-fold cross-validation procedure: First, trials were randomized in order and divided into 10 equal-sized folds; next, a leave-one-out procedure was used on the 10 folds, such that the classifier was trained on nine folds and tested on the remaining fold. This procedure was repeated 10 times until each fold was used exactly once for testing. Classifier performance was then averaged over folds. We applied between-class balancing using oversampling to ensure that, during training, the classifier would not develop a bias for the overrepresented class.

As a measure of classifier performance, we used the area under the curve (AUC), with the curve being the receiver operating curve of the cumulative probabilities that the classifier assigns to instances as coming from the same class (true positives) against the cumulative probabilities that the classifier assigns to instances that come from the other class (false positives). Importantly, the AUC was computed for each pairwise comparison between the correct class (i.e., correct location) and each of the five other classes, after which AUC values were averaged over the five pairwise comparisons. This procedure thus resulted in an AUC of 0.5, meaning chance-level classification performance. The AUC takes into account the degree of confidence (distance from the decision boundary) that the classifier has about class membership of individual instances, rather than averaging across binary decisions about class membership of individual instances (as happens when computing standard accuracy). As such, the AUC is considered a sensitive, nonparametric, and criterion-free measure of classification (Hand & Till, 2001). The distance from the decision boundary (i.e., classifier confidence score) of individual instances gives a single-trial measure of how much information there is in the EOG signals about the location of an item in the search display. At this point, these single-trial confidence scores were stored for within-participant correlation analyses with our neural EEG measures of interest (see subsection Exploratory Correlation Analyses of Time–Frequency Power—AUC). This decoding classification procedure was executed for every time point, thus yielding the evolution of classifier performance over time. Note that, as participants were allowed to make eye movements during the search task (and during the search task only), this analysis mainly reflects eye movements. However, the EOG channels presumably were also sensitive to systematic activity of the eye muscles caused by covert attention, for example, through microsaccades (Engbert & Kliegl, 2003), a premotor plan (Rizzolatti, Riggio, Dascola, and Umiltá, 1987), or movement inhibition (Munoz & Everling, 2004). Importantly, we do not make any claims about whether our EOG decoding results reflect either covert or overt attentional capture but rather investigate their combined effect, as a general index of attentional orienting.

Time–Frequency Decomposition

We decomposed the epoched EEG time series into their time–frequency representations using Morlet wavelet convolution for frequencies ranging from 1 to 40 Hz in 25 logarithmically spaced steps, using custom-writing MATLAB scripts. To create complex Morlet wavelets, a Gaussian ($e^{-t^2/2s^2}$), where s is the width of the Gaussian), was multiplied with 25 sine waves $e^{i2\pi ft}$, where i is the complex operator, f is frequency, and t is time. The Gaussian width was set as $s = \delta/(2\pi f)$, where δ represents the number of cycles of each wavelet, logarithmically spaced between 3 and 12 to have a good trade-off between temporal and frequency precision. Frequency-domain convolution was applied, that is, applying the fast Fourier transform to both the EEG data and the Morlet wavelets, multiplying them, and converting the result back to the time domain using the inverse fast Fourier transform. The squared magnitude of these complex signals was taken at each time point and each frequency to acquire power, that is, $[\text{real}(Z_t)^2 + \text{imag}(Z_t)^2]$. Power was further downsampled to 40 Hz to reduce computation time. Last, single-trial raw power was averaged over trials per condition, after which decibel normalization was applied per frequency and per channel [$\text{dB Power}_{tf} = 10*\log10(\text{Power}_{tf} / \text{Baseline Power}_f)$], with as baseline the condition-average power 500–200 msec before memory display onset. Note that this baseline period was used for the analysis of both the first and second delay periods.

Statistics

Behavioral Analysis

We analyzed behavior using Bayesian versions of paired-samples *t* tests or repeated-measures ANOVAs on both RT and accuracy data using JASP (Version 0.7.1.12, RRID: SCR_015823), a GUI-based software package for performing Bayesian statistics (Marsman & Wagenmakers, 2017). Bayesian hypothesis testing evaluates whether the data provide evidence in favor of either the alternative or null hypothesis, with the Bayes Factor (BF) being an interpretable numerical expression of this evidence (Wagenmakers et al., 2018; Rouder, Speckman, Sun, Morey, & Iverson, 2009).

EEG and EOG

We applied two lines of group-level statistics on the trial-averaged EEG results. First, as our hypothesis specifically pertained to (lateralized) posterior alpha power, we tested whether this signal would show sensitivity to template status (AT vs. AD) during both delay periods. For this analysis, we a priori selected the frequency range of 8–14 Hz and electrodes O1/2, PO3/4, and PO7/8, based on previous results (de Vries et al., 2018; de Vries, van Driel, & Olivers, 2017; van Driel, Gunseli, Meeter, & Olivers, 2017; van Ede, Niklaus, & Nobre, 2017). For the analysis of lateralized posterior alpha power, we subtracted ipsilateral from contralateral electrodes, whereas for the analysis of general (nonlateralized) posterior alpha power, we simply averaged over these six posterior electrodes. Second, on the basis of our previous findings, we hypothesized the involvement of a frontal, low-frequency cognitive control signal that would show sensitivity to template status (de Vries et al., 2018, 2019). However, given that our previous studies did not involve a distractor template, our current hypothesis did not pertain to a specific time interval, frequency band, or set of electrodes for this low-frequency signal. Therefore, we performed a mass-univariate statistical analysis on nonlateralized (i.e., irrespective of the memory cue location) power including all time–frequency–electrode points, to test if a specific frontal low-frequency cluster would dissociate between the AT and the AD. As statistical testing of EEG time or time–frequency signals involves many comparisons (each time, frequency, and/or electrode point), we performed group-level nonparametric permutation testing with cluster-based correction for multiple comparisons, which effectively controls for the autocorrelation over time, frequency, and space in the EEG signals (Maris, 2012; Maris & Oostenveld, 2007). We set the threshold for significance at a p value of .05 or lower (see Results section for the specific threshold per analysis). We performed 2,000 iterations and used the test statistic (i.e., t values) summed over all significant points belonging to the same cluster to define the respective cluster size. Only significant clusters larger than what can be expected by chance survive this procedure. For tests involving all electrodes, we used Fieldtrip's `ft_timelockstatistics.m` function with the method parameter set to "montecarlo" (Oostenveld et al., 2011; Maris & Oostenveld, 2007) and the `ft_prepare_neighbours.m` function with the method parameter set to "template" to define for each electrode which other electrodes are its neighbors. In the latter function, we set the minimum number of neighboring significant electrodes to define whether electrodes were part of the same cluster to 1. In our EEG analysis, we tested condition-average power or condition differences in power against baseline. Multivariate classification results of the EOG signals were tested at the group level for AUC deviations from chance (i.e., 0.5).

Exploratory Correlation Analyses of Time–Frequency Power—AUC

To further investigate the relevance of the template status-specific patterns of time–frequency power we observed during the delay periods and search tasks, we tested whether and how our two main neural signals of interest (i.e., posterior alpha power and frontal low-frequency power) related to specific patterns of attentional orienting during the search tasks, depending on the status of the template (i.e., target or distractor). We would like to emphasize that we did not a priori plan any of the following correlation analyses and, as such, they should be considered exploratory. We believe these correlation results merely provide additional support for our interpretation of the patterns in time–frequency power we observed.

Within-Participant Correlation

On the basis of the group-level classification (AUC) values for location decoding, we determined three time intervals of interest during each of the two search tasks, which we argued to specifically reflect the time windows of attentional orienting. For the AT condition, this interval was defined as the first time point at which the AUC values became significant for the target, until the AUC peak (see green line in Figure 3A). For the AD condition, we defined two time intervals, one from the first time point of significant AUC for the distractor until the following AUC peak (see orange line in Figure 3B) and one from the first time point of significant below-chance classification until the negative AUC peak (see black line in Figure 3C; i.e., after training the classifier on the AT template and testing it on the AD template). Given the pattern of classification observed for the AD (Figure 3B and 3C), we argued that these two intervals reflected two distinct cognitive mechanisms, namely, initial automatic (and unwanted) capture by the anticipated distractor and later volitional selection of the actual target on those trials. For that reason, we performed our correlation analyses on those two intervals separately. Furthermore, the reason for ending each interval at the AUC peak is that, after the peak, the likelihood of response increased rapidly, which consequently resulted in the removal of the search display

from the screen. On trials in which participants responded faster, AUC values dropped earlier (as the location information was no longer present), and posterior alpha power rose back to baseline earlier (as is generally the case when visual stimulation disappears). This resulted in a strongly significant negative correlation (data not shown) caused by differences in RTs rather than by a cognitive process of interest reflected by posterior alpha power.

After selecting the time windows, we averaged for each participant, condition, and single trial posterior alpha power within those time windows and correlated these raw, log-transformed power values across trials with the single-trial AUC confidence scores, also averaged over those time windows. This procedure resulted in within-participant correlation values, directly linking posterior alpha power to visual orienting and selection. We used Spearman's rank correlation, and coefficients were Fisher z-transformed to obtain normally distributed values before applying statistical group-level analyses (Silver & Dunlap, 1987). Next, we performed a similar within-participant correlation analyses between AUC values within those time windows and frontal low-frequency power directly after the auditory template status cue. That is, we averaged for each participant, condition, and single trial midfrontal theta power within the time–frequency–electrode cluster that showed a significant condition contrast ($p < .01$; see white outlines in Figure 6A) after the auditory cue that indicated the template status for the upcoming search task. Note that we selected the cluster at $p < .01$ to specifically capture the peak of the effect in midfrontal theta power. Using this procedure, we thus linked status cue-related midfrontal theta power to subsequent visual attentional orienting and selection during the search task.

Between-Participant Correlation

Last, we performed between-participant correlation analyses equivalent to the within-participant correlation analyses, except now between trial-averaged power and AUC values at the group level. That is, we selected the same time, frequency, and electrode points as described above, but now averaged for each participant and condition the trial-averaged power or AUC values within those selections. Furthermore, here, we performed a Bayesian version of a group-level correlation analysis, which resulted in a BF indicating the strength of evidence in favor of the alternative hypothesis of a significant correlation.

RESULTS

Behavior

On average, participants performed well on both search tasks, although slightly but reliably better on the second task, in terms of both accuracy (BF = 16; first search task: 90 ± 6%; second search task: 91 ± 5%; Figure 2A and 2B, top) and RTs (BF = 3.0×10^4; first search task: 1087 ± 144 msec; second search task: 974 ± 108 msec; Figure 2A and 2B, bottom). Importantly, search was both more accurate and faster for AT conditions than AD conditions, during both the first search task (accuracy: BF = 97; RT: BF = 1.4×10^9) and the second search task (accuracy: BF = 36; RT: BF = 9.9×10^7). We did not observe strong evidence for an interaction between template status (AT or AD) and position in the sequence (first or second search task), as the BF after adding an interaction to the model was only 2.5 times as high for accuracy (and only 1.3 times for RT) as without the interaction. To conclude, behavioral performance was better when observers could anticipate the target compared with when they could anticipate the distractor, consistent with previous findings (Beck, Luck, & Hollingworth, 2018; Becker, Hemsteger, &

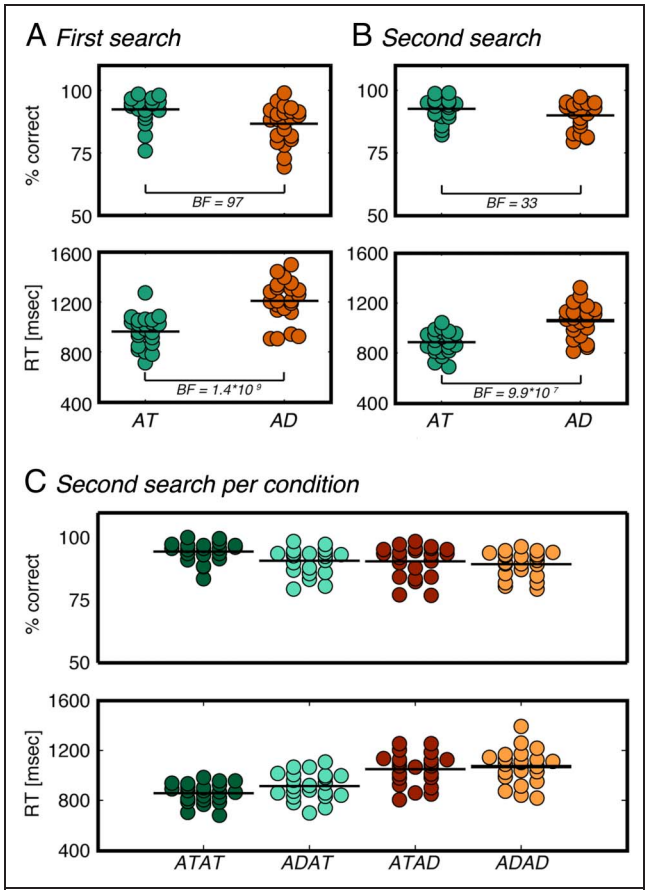

Figure 2. Behavioral results. In each subfigure, dots represent single-participant behavioral results (percentage correct and trial-averaged correct RT in each top and bottom panels, respectively). Horizontal line segments represent the group mean. Green and orange dots represent the AT and AD conditions, respectively. (A) First search task. (B) Second search task. (C) Results on the second search task for AT (green) and AD (orange), but separated based on template status during the first search task (indicated by shade: dark for AT and bright for AD).

Peltier, 2015; Kugler, 'T Hart, Kohlbecher, Einhäuser, & Schneider, 2015; Arita, Carlisle, & Woodman, 2012).

Location Decoding during Search

To better understand the observed lower performance for the anticipated distractors compared with the anticipated targets, we investigated attentional orienting toward both the anticipated color and the remaining, unanticipated color during search. To this end, we conducted MVPAs to decode the items' individual locations from the four EOG channels. Figure 3 shows that the individual locations of both colored items could be reliably classified within 180 msec after search display onset in both the AT and AD conditions. The location of the target in the AT condition could be significantly classified from 180 to 1670 msec and from 160 to 1630 msec after the onset of the first and second search displays, respectively ($p < .05$ cluster corrected; Figure 3A). In contrast, location decoding of the target in the AD condition showed a considerably delayed and wider distribution, resulting in higher AUC values for the target in the AT condition in the beginning of the search (200–830 and 160–690 msec for the first and second search, respectively; $p < .05$ cluster corrected) but higher AUC values for the target in the AD condition later in the search (980–1720 and

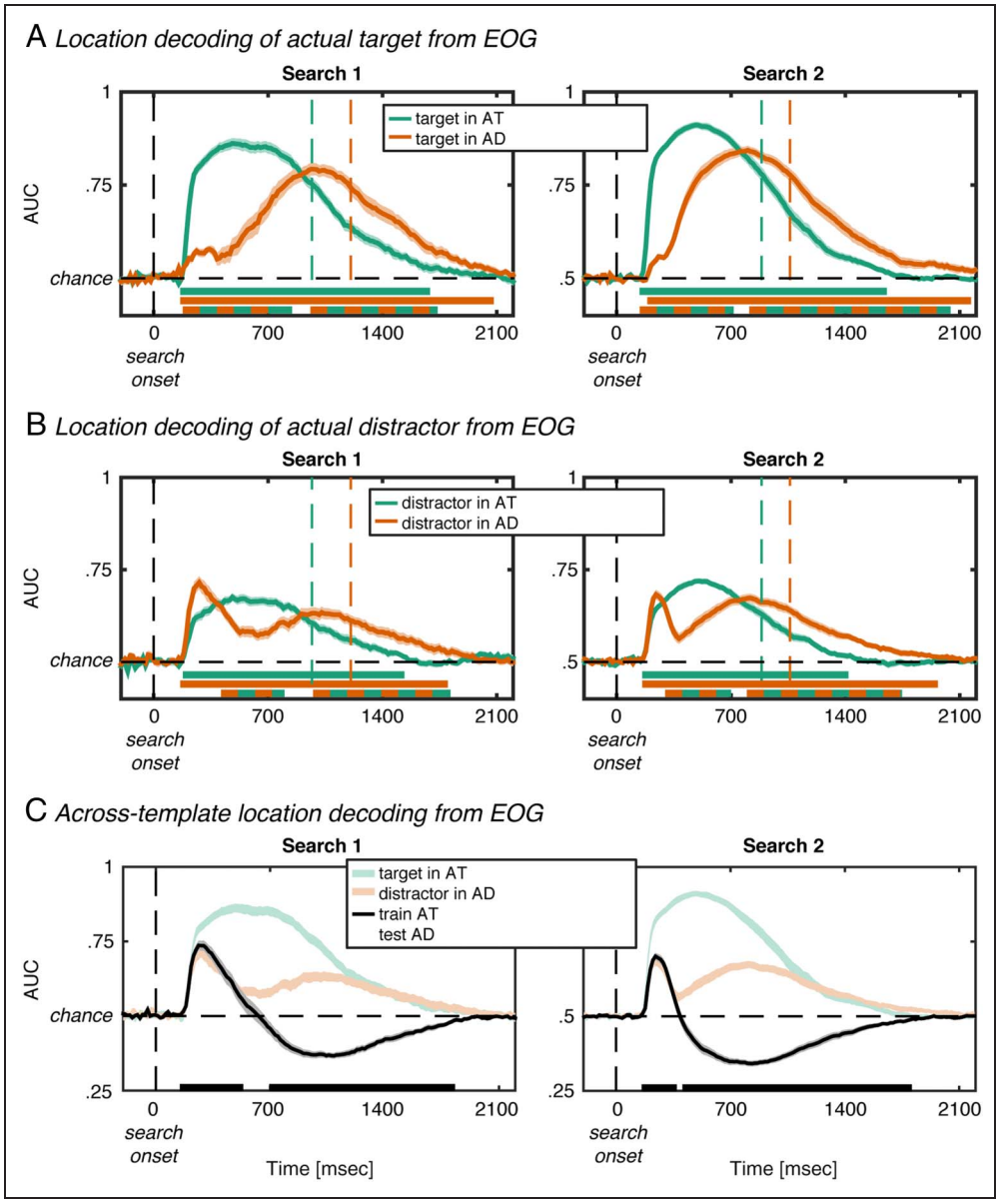

Figure 3. Decoding target and distractor location during search from EOG channels. (A) Classifier accuracy plotted over time for search target location decoding from the four EOG channels during the first search task (left column) and the second search task (right column). Note that the target was the anticipated color in the AT condition (green), whereas it was the remaining, unanticipated color in the AD condition (orange). Thick lines and shaded areas denote participant mean and *SEM*, respectively. The thick horizontal single-colored bars indicate time intervals of significant classification after cluster correction at $p < .05$, for the condition indicated with the same color. The thick horizontal double-colored bars indicate a significant condition difference in classification accuracy after cluster correction at $p < .05$. Vertical dashed lines indicate group-averaged RTs. (B) Same as A but now for decoding the location of the distractor. Note that the distractor color was the anticipated color in the AD condition (orange), whereas it was the remaining, unanticipated color in the AT condition (green). (C) The black line indicates classifier accuracy after training a classifier on the location of the anticipated color in the AT condition and testing it on the location of the anticipated color in the AD condition. For comparison, classifier accuracies for the anticipated color in the AT (green) and AD (orange) conditions (as taken from A and B) are plotted with 30% opacity. The initial above-chance across-template status decoding indicates a similar pattern of EOG activity, reflecting initial attentional orienting toward the anticipated color regardless of whether it is an anticipated target or distractor, whereas the later time interval of significant below-chance decoding indicates opposite patterns: Whereas attention is oriented toward the anticipated target color, it is oriented away from the anticipated distractor color.

830–2020 msec for the first and second search, respectively; $p < .05$ cluster corrected; Figure 3A). This delayed target selection when distractors are anticipated largely explains the lower performance compared with when targets are anticipated.

How about distractor selection? Under the advance inhibitory template account, one would expect a delayed or a reduced selection (and therefore location decoding) of the anticipated distractor. In contrast to that prediction, location decoding of the anticipated distractor showed an early sharp increase, which became significant ($p < .05$ cluster corrected) at 180 msec and reached an early peak at 280 msec (at 180 and 240 msec, respectively, for the second search task; Figure 3B). This early fast component could reflect automatic bottom–up capture by salient items (Theeuwes, 2010) or be in part driven by a general top–down attentional set for color (Found & Muller, 1996). However, classification accuracy during this first interval was higher for the anticipated distractor compared with the remaining, unanticipated color (200–450 and 180–300 msec for the first and second search, respectively; $p < .05$, although only the first search survived cluster correction; comparison not shown in Figure 3), indicating that attentional capture by the anticipated distractor rose above and beyond mere bottom–up capture by saliency or a general attentional set for color.

In addition, we observed a second time window of high decodability for the anticipated distractor later during the trial (Figure 3A and 3B). Training the classifier on the location of the anticipated target, but testing it on the location of the anticipated distractor, further unraveled the two separable components (Figure 3C). That is, whereas the pattern of EOG activity underlying the early peak in location decoding of the anticipated distractor was similar to location decoding of the anticipated target (i.e., significant above-chance across-template status location decoding from 170 to 510 msec and from 180 to 350 msec for the first and second search, respectively; $p < .05$ cluster corrected), the pattern of EOG activity underlying the later peak in location decoding was systematically dissimilar (i.e., significant below-chance across-template location decoding from 720 to 1810 msec and from 430 to 1790 msec for the first and second search, respectively; $p < .05$ cluster corrected). Together, these findings demonstrate an early fast component of attentional allocation toward the current content of working memory, whether target or distractor (cf. Olivers et al., 2006; Soto et al., 2005), and a second slow component, away from the anticipated distractor and toward the actual target instead (cf. Sawaki & Luck, 2013; Moher & Egeth, 2012). The initial capture of attention by the anticipated distractor further explains the delayed target selection and thus the lower performance compared with when the target can be anticipated (Figure 2). Taken together, these results speak against the advance inhibitory template hypothesis, to the extent that, if such inhibitory templates were set up at all, they were unsuccessful in preventing or even moderating attentional capture by anticipated distractors.

Lateralized Posterior Alpha Power not Sensitive to Template Status

Next, we investigated oscillatory mechanisms that have been related to differential priority assigned to items in working memory, and that may therefore differentiate between AT and AD templates. To this end, we tested whether lateralized posterior alpha (8–14 Hz) power was sensitive to template status. We previously found enhancement of alpha power contralateral to a working memory item that was not needed for the current perceptual task but instead was needed prospectively for a future task (de Vries et al., 2018), which we interpreted as preventing this currently irrelevant working memory from interacting with the current task. Because the AD template should be similarly prevented from interacting with attention during the search task, we expected an increase in contralateral alpha power for the AD relative to AT condition to appear toward the onset of the search display. Furthermore, because working memory representations may lead to involuntary attentional capture (Olivers et al., 2006; Soto et al., 2005), it would arguably be beneficial to maintain the AD template in a less active state compared with the AT template (de Vries et al., 2017). Consequently, we hypothesized relatively weaker contralateral alpha suppression during working memory encoding and initial maintenance for the AD template.

Not surprisingly, posterior alpha power was more suppressed (relative to baseline) for contralateral compared with ipsilateral electrodes, both during encoding and during the first delay period (325–725 msec relative to memory display onset, $p < .05$ cluster-corrected; Figure 4B, left column). Analysis of the full frequency range confirmed the peak of this effect to be localized to the alpha band (Figure 4A, left column). Stronger posterior alpha suppression contralateral compared with ipsilateral to the spatial location at which a memory item was presented is a common observation during working memory encoding and maintenance (Schneider, Mertes, & Wascher, 2015, 2016; Fukuda, Mance, & Vogel, 2015; Myers, Walther, Wallis, Stokes, & Nobre, 2015) and is interpreted as the selective processing of relevant sensory information through a reduction in alpha-induced "pulses" of inhibitory activity (Zumer et al., 2014; Jensen & Mazaheri, 2010; Klimesch et al., 2007). However, in contrast to our hypothesis, alpha lateralization was not sensitive to template status at any time during the first delay period (Figure 4B). Instead, Bayesian analysis of lateralized alpha power averaged over the significant condition-average cluster in the first delay (Figure 4B, left column, black bar), as well as Bayesian analysis of lateralized broadband power averaged over the significant time–frequency cluster of condition-average alpha lateralization in the first delay (Figure 4A, left column, black

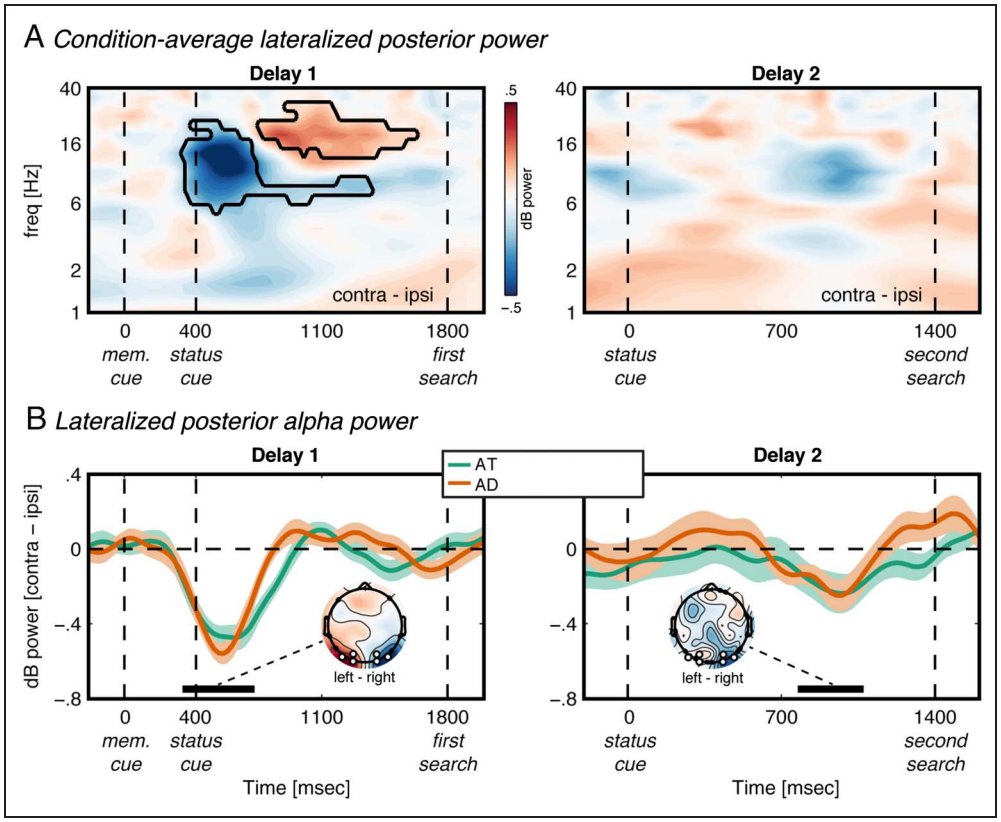

Figure 4. Lateralized posterior alpha power. (A) Condition-average time–frequency maps of lateralized (contralateral minus ipsilateral) power at the average of the a priori selected electrodes O1/2, PO3/4, and PO7/8 during the first delay period (left column; all trials) and the second delay period (right column; only those 50% of trials in which the first search task was omitted). Black outlines indicate a significant difference between contralateral and ipsilateral power at $p < .05$, cluster corrected. (B) Time series of lateralized alpha (8–14 Hz) power at the same electrodes as in A, for the AT (green) and the AD (orange). Thick lines and shaded areas denote participant mean and *SEM*, respectively. The horizontal black bars indicate significant condition-average alpha lateralization at $p < .05$, cluster corrected. There were no reliable effects of template status. The topographical maps illustrate the condition-average scalp distribution of alpha power in the significant time interval on trials with the memory item on the right subtracted from trials with the memory item on the left; black-bordered white disks mark the preselected electrodes. freq = frequency; contra = contralateral; ipsi = ipsilateral; mem. = memory.

outline around blue cluster), provided moderate evidence in favor of the null hypothesis of no condition difference (BF = 0.22 and BF = 0.31, respectively). Besides alpha lateralization, we also observed a significant condition-average lateralization of beta power, albeit in opposite direction (i.e., 14–29 Hz, 750–1625 msec; Figure 4A, left column, black outline around red cluster), with a similar posterior topographical distribution. Here too, Bayesian analysis provided moderate evidence against a condition difference (BF = 0.29). Beta-band power has recently been implicated in the endogenous activation of a cortical representation or a cognitive set, as well as decision-making or action selection (van Driel, Ort, Fahrenfort, & Olivers, 2019), all in service of current task demands (Spitzer & Haegens, 2017). As such, here, the hemisphere-specific beta signal may reflect a general decision or planning as to which action to perform when the anticipated information will be encountered. Alternatively, it could reflect the suppression of an oculomotor movement toward the location of the recently encoded working memory item (Engel & Fries, 2010). However, as this effect was unexpected and, furthermore, did not seem related to the question at hand (as there were no condition differences), we did not explore this effect further.

In the second delay period, a condition-average lateralization of alpha suppression reappeared (775–1075 msec relative to delay onset, $p < .05$ cluster-corrected; Figure 4B, right column). Such a reappearance of alpha lateralization after an intermittent task, in case of a working memory representation needed for an upcoming task, is consistent with earlier findings (de Vries et al., 2018, 2019; van Ede et al., 2017) and presumably reflects a shift of internal attention to retrieve or refresh the now newly task-relevant working memory representation. However, as in the first delay period, lateralized alpha suppression was not differentially modulated by template status, which was further supported by anecdotal evidence from a Bayesian t test on lateralized alpha power within the significant condition-average cluster (BF = 0.4).

Nonlateralized Posterior Alpha Power Regulates Perceptual Gating

As mentioned, we specifically hypothesized contralateral alpha enhancement for the anticipated distractor template in anticipation of search. However, as the anticipated distractor could appear anywhere in the search array, we next investigated the possibility that posterior alpha power would show a global, nonlateralized enhancement, that is, not locked to the location at which this template was originally presented. Indeed, in contrast to lateralized alpha power, overall, nonlateralized posterior alpha power was sensitive to the template status. Specifically, we observed relatively stronger posterior

alpha suppression for the AT compared with the AD at the start of the first search task (25–550 msec surrounding search onset; $p < .05$ cluster corrected; Figure 5B, left column) and before the start of the second search task (−125 to 150 msec surrounding search onset; $p < .05$ cluster corrected; Figure 5B, right column). Given the early onset of the condition contrast, this effect most likely reflects processes initiated before search, rather than in response to search display onset. Enhanced posterior alpha power for anticipated distractors is consistent with earlier observations of enhanced posterior alpha power when unknown distractors are expected to appear (Payne et al., 2013; Bonnefond & Jensen, 2012) and is generally interpreted as a mechanism to prevent interference by inhibiting or delaying perceptual processing as a whole (Payne & Sekuler, 2014; Bonnefond & Jensen, 2013; Foxe & Snyder, 2011). We speculate that also here such "closing of the gates to perception" would serve as an attempt to prevent the initial involuntary capture of attention by the anticipated distractor when target information is still uncertain (Figure 3B; also see Soto, Hodsoll, Rotshtein, & Humphreys, 2008). The fact that

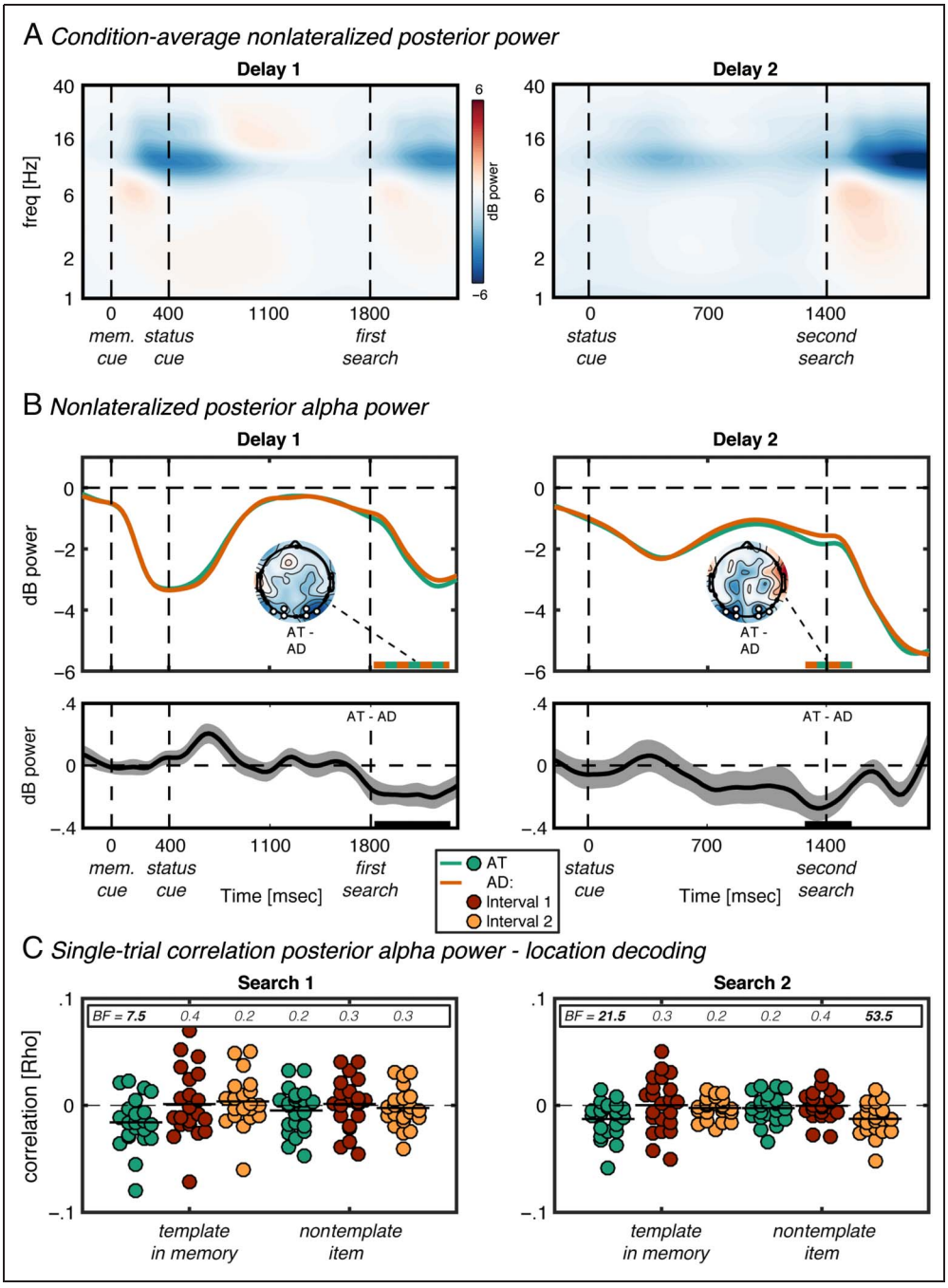

Figure 5. Nonlateralized posterior alpha power. (A) Condition-average time–frequency maps of nonlateralized power at the average of the a priori selected electrodes O1/2, PO3/4, and PO7/8 during the first delay period (left column; all trials) and the second delay period (right column; only those 50% of trials in which the first search task was omitted). (B) Time series of nonlateralized alpha (8–14 Hz) power at the same electrodes as in A, for the AT (green) and the AD (orange) conditions (top row) and for the condition contrast (bottom row). Thick lines and shaded areas denote participant mean and *SEM*, respectively. The horizontal double-colored (top row) and black (bottom row) bars indicate a significant condition difference at $p < .05$, cluster corrected. The topographical maps illustrate the condition difference in nonlateralized alpha power during the time interval in which this difference was significant; black-bordered white disks mark the preselected electrodes. (C) Within-participant correlation between nonlateralized posterior alpha power and single-trial classifier confidence scores for location decoding of the anticipated and unanticipated colors, during the time interval of an increase in location decoding accuracy (note that there are two intervals for location decoding of the AD; see Figure 3 and main text for details). Dots represent single-participant correlation values, whereas horizontal line segments represent the group mean. freq = frequency; mem. = memory.

the effect in alpha power was only present for the start of the search task further supports this proposition, as later during the trial observers will need to select the target. In contrast, the gates to perception can be fully opened when rapid selection of the relevant information is anticipated, as would be the case for anticipated targets. Such a perceptual gating mechanism would be consistent with the general selection suppression hypothesis.

To find additional support for our interpretation of the observed effect in posterior alpha power, we explored whether and how this nonlateralized effect on posterior alpha power at the start of the search related to attentional orienting as reflected by location decoding from the EOG channels, by correlating these measures at the single-trial level (see Methods). Interestingly, we observed a significant negative correlation between posterior alpha power and location classification performance for the AT in both search tasks (Figure 5C; BF = 7.5 and BF = 21.5 for the first and second search tasks, respectively). In other words, on trials in which posterior alpha power was more suppressed, the location of an anticipated target could be better classified. The same was true for the target in the AD condition albeit now only for the second search display (Figure 5C, right column; BF = 53.5; note that fewer trials contained a first search, which may have resulted in a lack of power here). Moreover, given the delayed selection of the target in this condition, this effect also occurred later, for the time window during which the target was selected. These correlation results indicate that, specifically, a stronger alpha suppression predicted better target localization. This supports the notion that general alpha suppression moderates how sensitive observers are to the perceptual input, with the gates opening up when fast target selection is anticipated, as is the case in the AT condition, whereas more strictly controlling input gating is the default when target information is still uncertain, as in the AD condition. Last, we ran an identical correlation analysis at the between-participant level, which did not show any significant effect (data not shown).

Midfrontal Theta as a Measure of Increased Cognitive Control for AD Templates

Next, we sought to identify which executive control mechanisms might support differential processing of anticipated distractors compared with anticipated targets. Because frontal low-frequency oscillations have been implicated in controlling a template status in working memory (de Vries et al., 2018, 2019), we hypothesized a similar functional role for controlling the specific template status in the current study as well. Because different studies using different paradigms report slightly different frequency bands and electrodes, we here tested the full time–space, by frequency–space, by electrode–space during both working memory delay periods for sensitivity to template status. We indeed observed the involvement of a strong midfrontal delta/theta cluster. Specifically, midfrontal delta-to-theta power increased more for AD than AT templates, during both the first delay period (1.5–7.5 Hz, 250–1150 msec; $p < .05$, cluster corrected; Figure 6A, left column) and the second delay period (2–16 Hz, −125 to 975 msec; $p < .05$, cluster corrected; Figure 6A, right column). Note that these intervals started somewhat before presentation of the status cue (which was at 400 and 0 msec in the first and second delay, respectively), which is most likely because of the fact that time–frequency decomposition through wavelet convolution inherently results in temporal smoothing, especially for lower frequencies. Additional analysis using a more stringent statistical threshold ($p < .01$) localized the peak of the effect after status cue presentation and mainly in the theta band (2–7.5 Hz, 450–900 msec and 5.5–8.5 Hz, 100–475 msec in the first and second delay periods, respectively; $p < .01$, although note that, at this stringent threshold, only the cluster in the first delay period survived correction for multiple comparisons).

Next, we explored whether and how this status cue-evoked frontal control signal related to attentional orienting during the search task. Interestingly, we found moderate-to-strong evidence for a negative across-participant correlation between midfrontal theta power during the first delay period and location classification for both anticipated and unanticipated colors, but exclusively so for the AD condition (Figure 6B, left column; BFs = 7.8 and 4.3 for the anticipated color in the first and second intervals and BFs = 14.2 and 1.4 for the remaining color in the first and second intervals, respectively). In other words, participants who demonstrated a stronger midfrontal theta increase in response to the auditory cue in the AD condition were less captured by any of the salient (i.e., colored) items during the subsequent search task. During the second delay period, the effects were similar, but statistically, the evidence was only anecdotal and occurred only for the actual target in the AD condition (i.e., the unanticipated item; Figure 6B, right column; BF = 2.8). Note however that, during the second delay, the template status may either remain the same or switch (see next section), and control signals may differ accordingly. Indeed, additional analyses on the effect of switching versus repeating of the template status between delay periods indicated that mainly switching from AT to AD (i.e., the ATAD condition) resulted in a relative increase in midfrontal theta power (Figure 7B) and, when running correlation analyses separately for this ATAD condition, there was indeed additional evidence for the negative correlation effect as we observed it during the first delay period (BF = 113; see subsection "Switching of template status between search tasks"). Identical correlation analyses, but at the single-trial level, did not show any significant effect (data not shown).

These results indicate that anticipated distractors come with increased cognitive control, as is reflected in stronger midfrontal theta power. The across-participant correlation

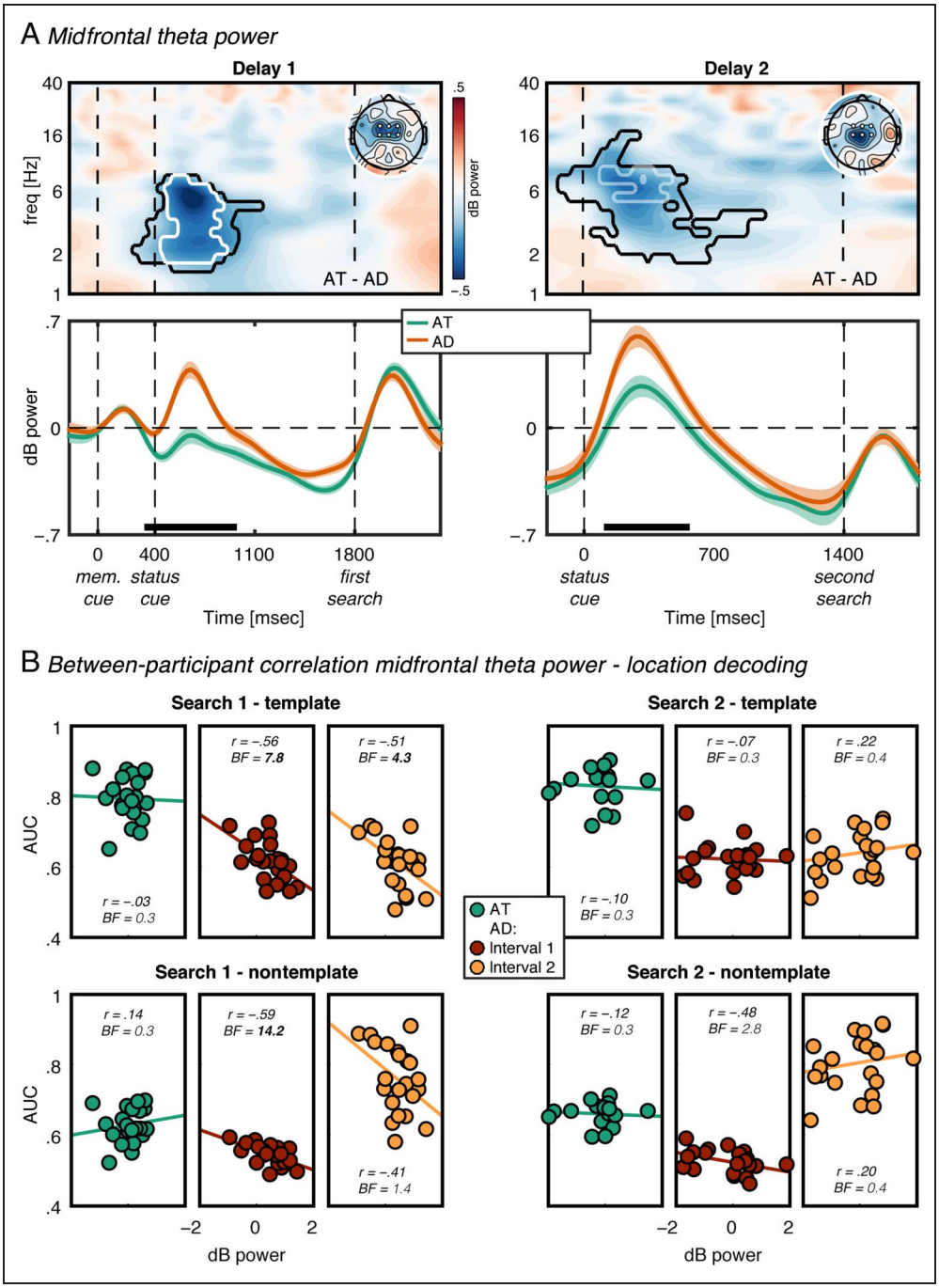

Figure 6. Midfrontal theta power. (A) Top: Time–frequency maps of the AT versus AD condition contrast for the first delay period (left column; all trials) and the second delay period (right column; only those 50% of trials in which the first search task was omitted), at the average of the electrodes indicated by black-bordered white disks in the inset topographical maps. The black and white outlines indicate clusters where this condition contrast was significant at $p < .05$ and $p < .01$, cluster corrected, respectively. The white outline in the time–frequency map of Delay 2 presented at 50% opacity indicates a condition contrast at $p < .01$, uncorrected. The inset topographical maps illustrate the averaged condition contrast within the white outlines in the corresponding time–frequency maps. Note that the six electrodes were merely selected for illustrative purposes; all 64 electrodes were included in the statistical test. Bottom: Same but for power averaged over the theta (4–8 Hz) frequency range. Black horizontal bars indicate a significant condition contrast at $p < .05$, cluster corrected. (B) Between-participant correlation between midfrontal theta power within the significant time–frequency–electrode cluster (at $p < .01$) and classification accuracy (AUC) for location decoding of the anticipated (top row) and unanticipated (bottom row) colors, during the time interval of increase in location decoding accuracy (see Figure 3; note that there are two intervals of AUC increase in the AD condition). Dots represent single-participant values, whereas diagonal line segments represent least-square fits. freq = frequency; mem. = memory.

analysis suggests that this leads to reduced attentional capture in general, whether by target or distractor, which may serve as a strategy to prevent interference from anticipated—and therefore difficult-to-ignore—distractors. This would further support the general selection suppression hypothesis. As such, the frontal control signals may have been the driving force behind the modulation of nonlateralized posterior alpha that we observed and that might serve the same purpose of general selection suppression by regulating the overall sensitivity to incoming signals. However, additional exploratory analyses did not reveal any correlation between the frontal and posterior signals (not shown here). This fits with the idea that posterior alpha suppression appears mainly tied to preparing for anticipated target selection, whereas the

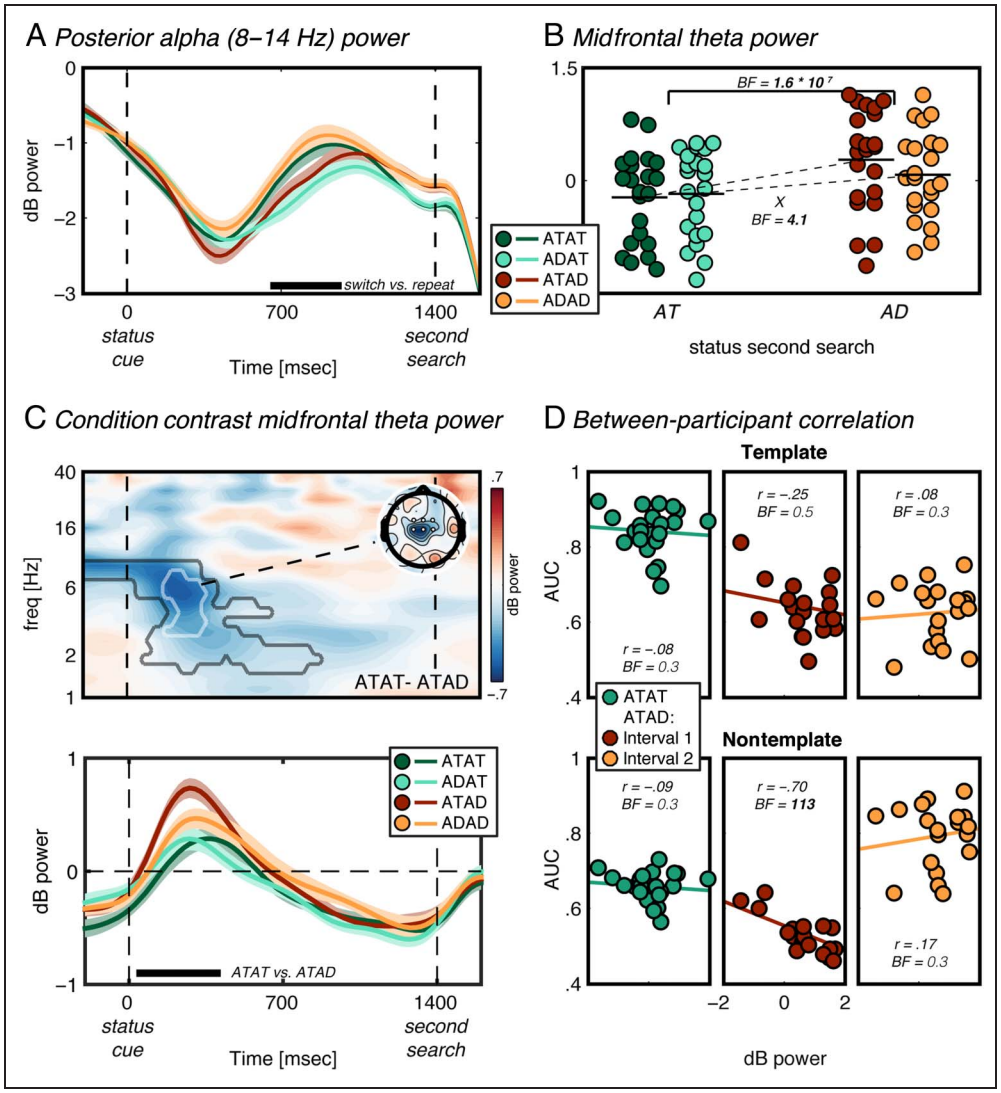

Figure 7. (A) Time series of nonlateralized alpha (8–14 Hz) power at the average of the a priori selected electrodes O1/2, PO3/4, and PO7/8 during the second delay period (only those 50% of trials in which the first search task was omitted), for the AT (green) and AD (orange) conditions, and separated based on template status during the first search task (indicated by shade: dark for AT and bright for AD). Thick lines and shaded areas denote participant mean and *SEM*, respectively. The horizontal black bar indicates a significant difference between trials in which the template status switched (ATAD and ADAT) versus repeated (ATAT and ADAD) in between search tasks at $p < .05$, cluster corrected. (B) Midfrontal theta power averaged over the time–frequency–electrode cluster showing a significant AT versus AD condition contrast (Figure 6A, right column, black outline) but illustrated separately for all four conditions as in A. The cross above a BF in the center of the figure indicates the interaction between template status during the first and second search tasks. (C) Top: Time–frequency map of the AT versus AD condition contrast, but only for those trials in which the template was the AT during the first search task (i.e., ATAT and ATAD), at the average of the electrodes indicated by black-bordered white disks in the topographical map. The black and white outlines presented at 50% opacity indicate a condition contrast uncorrected for multiple comparisons at $p < .05$ and $p < .01$, respectively. The topographical map illustrates the condition contrast averaged within the white outline in the time–frequency map. Note that these six electrodes were merely selected for illustrative purposes. All 64 electrodes were included in the statistical test. Bottom: Same but for power averaged over the theta (4–8 Hz) frequency range. Black horizontal bars indicate a significant condition contrast between ATAT and ATAD at $p < .05$, cluster corrected. (D) Between-participant correlation between midfrontal theta power within the significant time–frequency–electrode cluster (at $p < .01$, uncorrected) and classification accuracy (AUC) for location decoding of the anticipated (top row) and unanticipated (bottom row) colors, during the time interval of increase in location decoding accuracy (see Figure 3; note that there are two intervals of AUC increase in the AD condition). Only those trials in which the template was the AT during the first search task (i.e., ATAT and ATAD) were included in this analysis. Dots represent single-participant values, whereas diagonal line segments represent least-square fits. freq = frequency.

midfrontal theta activity is tied to preparing to suppress anticipated distractor selection.

Switching of Template Status between Search Tasks

Last, we investigated the effect of switching from one template status to the next, in between the two search tasks, on our neural measures of interest. First, we observed stronger nonlateralized posterior alpha power suppression in response to the second status cue when participants needed to switch between statuses compared with when the template status repeated (650–975 msec postcue; $p < .05$ cluster corrected; Figure 7A). A Bayesian ANOVA on this time window confirmed an interaction between search tasks (BF of the model including interaction was 48 times higher than the model without interaction), and post hoc pairwise comparisons revealed this effect to be driven by stronger alpha suppression for switching from AD to AT compared with repeating the AD status (i.e., ADAT vs. ADAD; BF = 53; light green and yellow lines in Figure 7A, respectively). Although we did not hypothesize this specific effect, we speculate it is again related to gating the perceptual input: When the first search

involved an anticipated distractor, the gates would remain relatively closed, as the observer attempts to prevent involuntary capture. When the same color is again a distractor in the second search, this state can be maintained. However, when the template status switches to an anticipated target on the second search task (i.e., ADAT), the gates can be fully opened, as is reflected in stronger alpha suppression.

In contrast, the stronger midfrontal theta increase for the AD condition compared with the AT condition in response to the second status cue was mainly driven by switching away from the AT status in the first search task and toward the AD status in the second search task (i.e., ATAD; Figure 7B). Indeed, a Bayesian ANOVA on condition-specific midfrontal theta power averaged over the time–frequency–electrode cluster showing a significant AT versus AD condition contrast (Figure 6A, right column, black outline) confirmed moderate evidence for an interaction between search tasks (BF of the model including interaction was 4.1 times higher than the model without interaction). A permutation test over all time, frequency, and electrode points showed a relative increase in midfrontal theta power for ATAD relative to ATAT (Figure 7C, black and white outline for $p < .05$ and $p < .01$, respectively, although uncorrected), very similar to what we observed for the combined conditions (AD vs. AT in the second delay; Figure 6A, right column). Last, when rerunning our across-participant correlation analyses (Figure 6B, right column), but now only including the ATAT and ATAD conditions, we found additional evidence for a negative correlation between midfrontal theta power and location decoding, but exclusively so for the actual target when the distractor was anticipated (Figure 7D; BF = 113 for the unanticipated item). That is, participants who exhibited a stronger midfrontal theta increase during the second delay in the ATAD condition were less captured by the actual target in the second search task. These results again support the idea that specifically setting the template as an AD involves an increase in midfrontal theta power and that the midfrontal theta increase is mainly involved in initializing a general inhibitory state, to prevent attentional capture in the subsequent search display. In contrast, when observers know what the target will be, they lower sensory thresholds, as indicated by posterior alpha suppression.

DISCUSSION

We investigated the oscillatory dynamics that underlie one of the key characteristics of visual selection: How do we prepare to ignore a known distractor, and how does this differ mechanistically from preparing to select a known target? We measured EEG while participants memorized a color for two subsequent search tasks, each preceded by a delay period, with an auditory cue at each delay onset signaling whether the template would serve as a target or distractor on the corresponding search task. Furthermore, we investigated attentional allocation during search by means of target and distractor location decoding from four EOG channels. We report a number of important findings. First, any item matching the template held in working memory, including the anticipated distractor, automatically attracted attention early during search. Only after this initial allocation, attention was oriented away from an anticipated distractor and toward the actual target, suggesting that the anticipated distractor could not initially be avoided. Second, search-related nonlateralized posterior alpha power was relatively suppressed for the anticipated target compared with the anticipated distractor, and this suppression selectively predicted attentional selection of the target, indicating that observers upregulate perceptual sensitivity in response to known target information. Conversely, observers downregulate perceptual sensitivity when the target is as yet unknown. Third, delay period midfrontal theta power was relatively enhanced for the anticipated distractor conditions and, moreover, predicted participants' inhibition of initial attentional capture by this distractor, at the expense of also suppressing capture by the actual target in that condition. Together, our findings are consistent with the general selection suppression and reactive reorienting hypotheses, not with the advance inhibitory template hypothesis.

No Evidence for an Advance Inhibitory Template

Our results provide evidence against a working-memory-based advance inhibitory template account. First, the EOG data demonstrate that, initially, attention is oriented toward the anticipated distractor rather than away from it, with initially very similar selection patterns for anticipated targets and anticipated distractors. In fact, anticipated distractor selection was stronger than for any unanticipated but equally salient color, indicating that the stronger capture was specific to the distractor being maintained in memory. Although we did not measure actual eye movements, location decoding from the EOG channels was very effective with high classification accuracy, revealing two clearly dissociable components of attentional allocation for anticipated distractors. Furthermore, our measure may be argued to be more sensitive in this respect as it presumably captures not only eye movements but also systematic activity of the eye muscles caused by covert attentional allocation through any premotor plan (Rizzolatti et al., 1987) or movement inhibition (Munoz & Everling, 2004). Although this remains to be validated in studies that separately measure overt eye movements, we argue that the here used measure of location decoding provides a useful index of the combination of overt and covert attentional orienting.

Second, another hallmark of an advance inhibitory template is that processing of the specific sensory memory representation should be inhibited before search. One would therefore predict posterior alpha enhancement selectively for the retinotopic location at which

the anticipated distractor is processed (Schneider et al., 2019; de Vries et al., 2018). Contrary to this, we found the same pattern of lateralized posterior alpha power for anticipated targets and anticipated distractors during the delay period before search. Of course, it could be that our measure of lateralized posterior alpha power is not sensitive to differences in sensory processing here; nevertheless, we believe that this set of results provides converging evidence against the advance inhibitory template hypothesis.

Instead, our location decoding results point toward reactive reorienting after observers have selected the distractor, consistent with previous findings (Sawaki & Luck, 2013; Moher & Egeth, 2012). Moher and Egeth (2012) proposed that this initial selection of the distractor might be part of a strategic "seek and destroy" mechanism, in which the distractor is first selected to more efficiently ignore it afterward. However, recently, Beck and colleagues provided evidence against this (Beck et al., 2018), as they found that initial oculomotor capture by an anticipated distractor did not predict the amount of avoidance later during that trial. Furthermore, if selection of the anticipated distractor were strategic, one would not expect increased perceptual gating as observed here in the posterior alpha power signal. In our view, a more likely explanation is that selection of input matching the current activated content of working memory may be automatic and largely unavoidable, even when unwanted (Soto et al., 2008). Observers then have to reactively suppress the accidentally selected distractor. Such reactive suppression is also suggested by ERP studies that show that attentional selection of a salient distractor, as indicated by the N2pc, is often followed by the Pd, an ERP measure of distractor suppression (Liesefeld, Liesefeld, Töllner, & Müller, 2017; Sawaki & Luck, 2013; Hilimire, Mounts, Parks, & Corballis, 2009).

This is not to say that advance suppression cannot occur. First, there is ample behavioral and neuroscientific evidence for the anticipatory suppression of perceptual processing at an expected distractor location (Dube, Basciano, Emrich, & Al-Aidroos, 2016; Al-Aidroos, Emrich, Ferber, & Pratt, 2012; Händel et al., 2011; Munneke, Van der Stigchel, & Theeuwes, 2008; Rihs et al., 2007; Ruff & Driver, 2006; Serences, Yantis, Culberson, & Awh, 2004), but this does not demonstrate the feature-based, distractor-specific advance inhibition that we were after here. A previous report that claimed such advance feature-based inhibition (Arita et al., 2012) may have contaminated the to-be-ignored feature with a consistent spatial location (Beck & Hollingworth, 2015; Becker et al., 2015).

Second, advance suppression may occur through implicit or long-term memory. A number of studies have observed behavioral benefits after repeating the same distractor location or feature over many trials, rather than providing information on a trial-by-trial basis (Gaspelin & Luck, 2019; Stilwell & Vecera, 2018; Wang & Theeuwes, 2018a, 2018b; Cunningham & Egeth, 2016; Leber, Gwinn, Hong, & O'Toole, 2016; Noonan et al., 2016). Similarly, some EEG studies found the Pd component instead of rather than following the N2pc, which would be consistent with the distractor not being initially attended, and would thus reflect proactive suppression (e.g., Gaspelin & Luck, 2018a; Weaver, van Zoest, & Hickey, 2017; Sawaki & Luck, 2010). However, in these Pd studies, the distractor feature was typically kept constant over many trials (Gaspelin & Luck, 2018a; Weaver et al., 2017; Gaspar, Christie, Prime, Jolicœur, & McDonald, 2016; Gaspar & McDonald, 2014; Kiss, Grubert, Petersen, & Eimer, 2012; Hickey, Di Lollo, & McDonald, 2009). Consistent with a signal suppression model (Sawaki & Luck, 2010), these findings indicate that advance suppression of the feature-specific signal is possible when the distracting feature is learned. In contrast to our working memory model, this type of repetition suppression presumably involves a more automatic desensitization or reduction of the distractor-evoked neural activity (Noonan et al., 2018; Summerfield, Trittschuh, Monti, Mesulam, & Egner, 2008), driven by unconscious selection history or implicit priming (Gaspelin, Gaspar, & Luck, 2019; Gaspelin & Luck, 2018b). Indeed, behavioral evidence suggests that, although it is possible to implicitly learn to proactively suppress specific distractor features, this ability disappears when explicitly cued on a trial-by-trial basis on the distractor features (Stilwell & Vecera, 2018). In the current study, we specifically sought to investigate if working memory can be utilized to suppress specific distractor features in advance, before display onset, when cued on a trial-by-trial basis. On the basis of our own results and the existing literature, we conclude that the evidence weighs against advance working-memory-based templates of an inhibitory nature (i.e., templates for rejection).

Increased Cognitive Control and Perceptual Gating Indicate General Selection Inhibition

Interestingly, we did observe activity that differentiated between AT and AD conditions, also already before search onset. However, these signals were not item specific and appeared to be geared to regulating perceptual processing in general. First, we observed a robust increase in midfrontal theta power for anticipated distractors already early during the delay period. We previously observed a similar signature of cognitive control to be consistently involved in the anticipatory prioritization of working memory representations depending on the imminent perceptual goals of the observer (de Vries et al., 2018, 2019). However, whereas that neural response was specifically localized to the delta (2–4 Hz) frequency range and in electrodes above frontal cortex (i.e., around AFz), the current signal was more centrally localized (i.e., around FCz/Cz) and occurred in a slightly higher theta frequency range. Interestingly, this exact spatio-spectral signature of midfrontal theta power is very well established in the cognitive control literature and is proposed to reflect the detection of conflict in pFC, which subsequently

signals the need for increased control to dorsolateral pFC, which in turn implements increased control in task-relevant sensory areas (Janssens, De Loof, Boehler, Pourtois, & Verguts, 2018; Cavanagh & Frank, 2014; Cohen, 2014a). For example, a relative increase in midfrontal theta power is observed in response to incongruent versus congruent response options (Cavanagh & Frank, 2014), and relevant for the matter at hand, it has been observed that midfrontal theta increases during prestimulus intervals when conflict is anticipated (van Driel, Swart, Egner, Ridderinkhof, & Cohen, 2015) and occurs in response to changing search targets (van Driel, Ort, et al., 2019), and it is stronger on incongruent trials if the previous trial was congruent rather than incongruent (van Driel et al., 2015). Similar to this previous trial effect, we also here mainly observed a midfrontal theta increase in the second delay period if the target was anticipated on the first search task and not if the distractor was anticipated, suggesting that this cognitive control state only needs to be initialized once for that particular working memory representation. Given the abundance of literature demonstrating this specific midfrontal theta signal in relation to processing conflict, we speculate our results to reflect an internal conflict between the activation of a working memory representation that is expected to automatically draw attention toward matching input (Soto et al., 2008; Olivers et al., 2006) and a cue signaling at the same time that this should be avoided. Furthermore, we found that this increase in midfrontal theta power predicted a reduction in attentional capture, although not only by the anticipated distractor but also by the actual target in that condition (i.e., the unanticipated item). Taken together, we argue that the here observed frontal low-frequency signature reflects a general increase in cognitive control after conflicting information, rather than being related to prioritizing a specific working memory representation (as in de Vries et al., 2018).

In addition, we found that, around search display onset, overall nonlateralized posterior alpha power was more suppressed for anticipated targets than for anticipated distractors. Furthermore, this alpha suppression predicted attentional selection of the target on a single-trial level, during early selection for the anticipated target as well as during later selection of the unanticipated target in trials in which the distractor was anticipated. It also occurred when observers switched from an anticipated distractor in the first search to an anticipated target in the second search. These findings are consistent with a perceptual gating account in which posterior alpha suppression upregulates perceptual sensitivity to expected input and, conversely, posterior alpha enhancement inhibits selection and processing of irrelevant information by perceptual gating (Payne & Sekuler, 2014 Bonnefond & Jensen, 2013; Foxe & Snyder, 2011). This is similar to the expectation suppression account of distractor suppression (Noonan et al., 2018), which states that an inhibitory state suppressing all expected perceptions is the status quo and is only released when a top–down signal for the target is present. Although our results do not provide conclusive evidence for which functional mechanism of perceptual control plays a key role (i.e., alpha suppression for the anticipated target, alpha enhancement for the anticipated distractor, or both), they do demonstrate a relative "closing of the gates to perception" when an anticipated distractor is activated in working memory.

The fact that the alpha power modulation was present above the whole visual cortex independent of the sensory region in which the anticipated distractor was processed (i.e., nonlateralized) suggests that it pertains to all incoming visual input. Consistent with such a general gating mechanism, recent fMRI studies reported a general reduction in BOLD activity in early visual cortex for anticipated distractors compared with anticipated targets (Reeder, Olivers, & Pollmann, 2017), without this decrease being distinctive for specific distractor features (Reeder et al., 2018). We argue the current results to reflect increased perceptual gating in an attempt to prevent involuntary perceptual selection of anticipated distractors, which moreover explains that the time taken to initiate the first eye movement during search is longer for anticipated distractors than anticipated targets (Beck et al., 2018). Taken together, these findings speak to a general selection suppression account, rather than an item-specific, advance inhibitory template within working memory.

Strategic Attending

One potential caveat of our experimental design might lead to observers strategically attending the distractor. Note that, on anticipated distractor trials, participants identified the actual target in the search display on the basis of it being the only other colored item besides the known distractor. Therefore, participants required the anticipated distractor to perform the task, necessitating some form of active storage. As such, this design may have discouraged advance inhibition of the memory item and instead may have encouraged a strategy whereby participants first identified the only item in memory and then attended to the other item as the target. One could argue that a more optimal design is one in which participants would not need to use the anticipated distractor in any way to perform the task and that an advance inhibitory template might still emerge under such conditions. Although we cannot exclude this possibility, we can argue against it on two grounds. First, for the current research question, any experimental design needs to fulfill certain criteria. Most importantly, to allow for a clean comparison of the EEG signals related to advance processing of anticipated targets versus anticipated distractors, all other circumstances need to be as similar as possible. Preparation for the search display should thus involve either the anticipated target or the anticipated distractor,

with a similar memory load. Moreover, the other item then needs to be unknown to prevent recoding distractor information into target information or vice versa. Given these constraints, we believe the current design came close to optimal.

Second, we conjecture that the argument of observers needing the distractor is rather circular. It relies heavily on the assumption that advance suppression of the distractor would not be helpful—after all, one needs the distractor to identify the target. However, had observers been able to successfully suppress the distractor in advance, then there would be no need to identify it first, because the target would then automatically have been the item with the highest priority in the display. Therefore, we argue that, if an advance inhibitory template would be a viable strategy, we would have found evidence for it, also with the current design.

Relatedly, one could argue that our design may have stimulated a strategy of engaging a "singleton detection mode" (Leber & Egeth, 2006; Bacon & Egeth, 1994), over one using an advance inhibitory template. If a singleton detection mode would be engaged, attention would be automatically drawn toward any of the two distinct colors (singletons) in the search display. However, this explanation of the results seems unlikely for two reasons. First, in anticipated distractor trials, attention was captured more strongly by the memory-matching color than by the only other color (the actual target) in the search display, demonstrating that observers were activating a specific feature, although it belonged to the distractor. Second, participants simply could not perform the task correctly by solely using a singleton detection mode. In addition, a second phase engaging a feature activation or deactivation mode, depending on information in working memory, would be required. Because the anticipated distractor initially captured attention, our results demonstrate that this feature deactivation does not start in advance.

Conclusion

In the current study, we set out to address how we prepare for anticipated distractors. We found no evidence for item-specific advance suppression. Instead, we provide evidence that actively preparing for a distractor results in an internal conflict between the goal of maintaining the item and the goal of subsequently ignoring it. Remembering the distractor actually leads to increased initial distraction. In an attempt to prevent "looking at the white bear," the system initiates a general inhibitory strategy to suppress all attentional selection by increasing perceptual gating.

Acknowledgments

I. E. J. d. V., E. S., J. v. D., and C. N. L. O. designed the research; I. E. J. d. V. and E. S. performed the research; I. E. J. d. V. and E. S. analyzed the data; and I. E. J. d. V., J. v. D., and C. N. L. O. wrote the article. This work was supported by the European Research Council Consolidator grant (ERC-2013-CoG-615423) to C. N. L. O. The authors declare no competing financial interests.

Reprint requests should be sent to Ingmar E. J. de Vries, Department of Experimental and Applied Psychology, Faculty of Behavioural and Movement Sciences, Vrije Universiteit Amsterdam, Van der Boechorststraat 1, 1081BT, Amsterdam, Netherlands, or via e-mail: i.e.j.de.vries@vu.nl.

REFERENCES

Al-Aidroos, N., Emrich, S. M., Ferber, S., & Pratt, J. (2012). Visual working memory supports the inhibition of previously processed information: Evidence from preview search. *Journal of Experimental Psychology: Human Perception and Performance*, *38*, 643–663.

Arita, J. T., Carlisle, N. B., & Woodman, G. F. (2012). Templates for rejection: Configuring attention to ignore task-irrelevant features. *Journal of Experimental Psychology: Human Perception and Performance*, *38*, 580–584.

Bacon, W. F., & Egeth, H. E. (1994). Overriding stimulus-driven attentional capture. *Perception & Psychophysics*, *55*, 485–496.

Beck, V. M., & Hollingworth, A. (2015). Evidence for negative feature guidance in visual search is explained by spatial recoding. *Journal of Experimental Psychology: Human Perception and Performance*, *41*, 1190–1196.

Beck, V. M., Luck, S. J., & Hollingworth, A. (2018). Whatever you do, don't look at the…: Evaluating guidance by an exclusionary attentional template. *Journal of Experimental Psychology: Human Perception and Performance*, *44*, 645–662.

Becker, M. W., Hemsteger, S., & Peltier, C. (2015). No templates for rejection: A failure to configure attention to ignore task-irrelevant features. *Visual Cognition*, *23*, 1150–1167.

Bonnefond, M., & Jensen, O. (2012). Alpha oscillations serve to protect working memory maintenance against anticipated distracters. *Current Biology*, *22*, 1969–1974.

Bonnefond, M., & Jensen, O. (2013). The role of gamma and alpha oscillations for blocking out distraction. *Communicative and Integrative Biology*, *6*, e22702.

Bundesen, C. (1990). A theory of visual attention. *Psychological Review*, *97*, 523–547.

Cavanagh, J. F., & Frank, M. J. (2014). Frontal theta as a mechanism for cognitive control. *Trends in Cognitive Sciences*, *18*, 414–421.

Cohen, M. X. (2014a). A neural microcircuit for cognitive conflict detection and signaling. *Trends in Neurosciences*, *37*, 480–490.

Cohen, M. X. (2014b). *Analyzing neural time series data: Theory and practice*. Cambridge, MA: MIT Press.

Cunningham, C. A., & Egeth, H. E. (2016). Taming the white bear: Initial costs and eventual benefits of distractor inhibition. *Psychological Science*, *27*, 476–485.

de Vries, I. E. J., van Driel, J., Karacaoglu, M., & Olivers, C. N. L. (2018). Priority switches in visual working memory are supported by frontal delta and posterior alpha interactions. *Cerebral Cortex*, *28*, 4090–4104.

de Vries, I. E. J., van Driel, J., & Olivers, C. N. L. (2017). Posterior alpha EEG dynamics dissociate current from future goals in working memory guided visual search. *Journal of Neuroscience*, *37*, 1591–1603.

de Vries, I. E. J., van Driel, J., & Olivers, C. N. L. (2019). Decoding the status of working memory representations in preparation of visual selection. *Neuroimage*, *191*, 549–559.

Delorme, A., & Makeig, S. (2004). EEGLAB: An open source toolbox for analysis of single-trial EEG dynamics including

independent component analysis. *Journal of Neuroscience Methods*, *134*, 9–21.
Derrington, A. M., Krauskopf, J., & Lennie, P. (1984). Chromatic mechanisms in lateral geniculate nucleus of macaque. *Journal of Physiology*, *357*, 241–265.
Desimone, R., & Duncan, J. (1995). Neural mechanisms of selective visual attention. *Annual Review of Neuroscience*, *18*, 193–222.
Dube, B., Basciano, A., Emrich, S. M., & Al-Aidroos, N. (2016). Visual working memory simultaneously guides facilitation and inhibition during visual search. *Attention, Perception, & Psychophysics*, *78*, 1232–1244.
Duncan, J., & Humphreys, G. W. (1989). Visual search and stimulus similarity. *Psychological Review*, *96*, 433–458.
Engbert, R., & Kliegl, R. (2003). Microsaccades uncover the orientation of covert attention. *Vision Research*, *43*, 1035–1045.
Engel, A. K., & Fries, P. (2010). Beta-band oscillations-signalling the status quo? *Current Opinion in Neurobiology*, *20*, 156–165.
Fahrenfort, J. J., van Driel, J., van Gaal, S., & Olivers, C. N. L. (2018). From ERPs to MVPA using the Amsterdam Decoding and Modeling toolbox (ADAM). *Frontiers in Neuroscience*, *12*, 368.
Found, A., & Muller, H. J. (1996). Searching for unknown feature targets on more than one dimension: Investigating a "dimension-weighting" account. *Perception & Psychophysics*, *58*, 88–101.
Foxe, J. J., & Snyder, A. C. (2011). The role of alpha-band brain oscillations as a sensory suppression mechanism during selective attention. *Frontiers in Psychology*, *2*, 154.
Fukuda, K., Mance, I., & Vogel, E. K. (2015). α Power modulation and event-related slow wave provide dissociable correlates of visual working memory. *Journal of Neuroscience*, *35*, 14009–14016.
Gaspar, J. M., Christie, G. J., Prime, D. J., Jolicœur, P., & McDonald, J. J. (2016). Inability to suppress salient distractors predicts low visual working memory capacity. *Proceedings of the National Academy of Sciences, U.S.A.*, *113*, 3693–3698.
Gaspar, J. M., & McDonald, J. J. (2014). Suppression of salient objects prevents distraction in visual search. *Journal of Neuroscience*, *34*, 5658–5666.
Gaspelin, N., Gaspar, J. M., & Luck, S. J. (2019). Oculomotor inhibition of salient distractors: Voluntary inhibition cannot override selection history. *Visual Cognition*, *27*, 227–246.
Gaspelin, N., & Luck, S. J. (2018a). Combined electrophysiological and behavioral evidence for the suppression of salient distractors. *Journal of Cognitive Neuroscience*, *30*, 1265–1280.
Gaspelin, N., & Luck, S. J. (2018b). The role of inhibition in avoiding distraction by salient stimuli. *Trends in Cognitive Sciences*, *22*, 79–92.
Gaspelin, N., & Luck, S. J. (2019). Inhibition as a potential resolution to the attentional capture debate. *Current Opinion in Psychology*, *29*, 12–18.
Gayet, S., Guggenmos, M., Christophel, T. B., Haynes, J.-D., Paffen, C. L. E., Van der Stigchel, S., et al. (2017). Visual working memory enhances the neural response to matching visual input. *Journal of Neuroscience*, *37*, 6638–6647.
Gazzaley, A., & Nobre, A. C. (2012). Top–down modulation: Bridging selective attention and working memory. *Trends in Cognitive Sciences*, *16*, 129–135.
Geng, J. J. (2014). Attentional mechanisms of distractor suppression. *Current Directions in Psychological Science*, *23*, 147–153.
Groppe, D. M., Makeig, S., & Kutas, M. (2009). Identifying reliable independent components via split-half comparisons. *Neuroimage*, *45*, 1199–1211.
Hand, D. J., & Till, R. J. (2001). A simple generalisation of the area under the ROC curve for multiple class classification problems. *Machine Learning*, *45*, 171–186.
Händel, B. F., Haarmeier, T., & Jensen, O. (2011). Alpha oscillations correlate with the successful inhibition of unattended stimuli. *Journal of Cognitive Neuroscience*, *23*, 2494–2502.
Harrison, S. A., & Tong, F. (2009). Decoding reveals the contents of visual working memory in early visual areas. *Nature*, *458*, 632–635.
Helfrich, R. F., Huang, M., Wilson, G., & Knight, R. T. (2017). Prefrontal cortex modulates posterior alpha oscillations during top–down guided visual perception. *Proceedings of the National Academy of Sciences, U.S.A.*, *114*, 9457–9462.
Hickey, C., Di Lollo, V., & McDonald, J. J. (2009). Electrophysiological indices of target and distractor processing in visual search. *Journal of Cognitive Neuroscience*, *21*, 760–775.
Hilimire, M. R., Mounts, J. R., Parks, N. A., & Corballis, P. M. (2009). Competitive interaction degrades target selection: An ERP study. *Psychophysiology*, *46*, 1080–1089.
Itti, L., & Koch, C. (2001). Computational modelling of visual attention. *Nature Reviews Neuroscience*, *2*, 194–203.
Janssens, C., De Loof, E., Boehler, C. N., Pourtois, G., & Verguts, T. (2018). Occipital alpha power reveals fast attentional inhibition of incongruent distractors. *Psychophysiology*, *55*, e13011.
Jensen, O., & Mazaheri, A. (2010). Shaping functional architecture by oscillatory alpha activity: Gating by inhibition. *Frontiers in Human Neuroscience*, *4*, 186.
Jensen, O., & Tesche, C. D. (2002). Frontal theta activity in humans increases with memory load in a working memory task. *European Journal of Neuroscience*, *15*, 1395–1399.
Johnson, E. L., Dewar, C. D., Solbakk, A. K., Endestad, T., Meling, T. R., & Knight, R. T. (2017). Bidirectional frontoparietal oscillatory systems support working memory. *Current Biology*, *27*, 1829–1835.
Kayser, J., & Tenke, C. E. (2015). On the benefits of using surface Laplacian (current source density) methodology in electrophysiology. *International Journal of Psychophysiology*, *97*, 171–173.
Kiss, M., Grubert, A., Petersen, A., & Eimer, M. (2012). Attentional capture by salient distractors during visual search is determined by temporal task demands. *Journal of Cognitive Neuroscience*, *24*, 749–759.
Klimesch, W., Sauseng, P., & Hanslmayr, S. (2007). EEG alpha oscillations: The inhibition-timing hypothesis. *Brain Research Reviews*, *53*, 63–88.
Kugler, G., 'T Hart, B. M., Kohlbecher, S., Einhäuser, W., & Schneider, E. (2015). Gaze in visual search is guided more efficiently by positive cues than by negative cues. *PLoS One*, *10*, e0145910.
Leber, A. B., & Egeth, H. E. (2006). It's under control: Top–down search strategies can override attentional capture. *Psychonomic Bulletin & Review*, *13*, 132–138.
Leber, A. B., Gwinn, R. E., Hong, Y., & O'Toole, R. J. (2016). Implicitly learned suppression of irrelevant spatial locations. *Psychonomic Bulletin & Review*, *23*, 1873–1881.
Liesefeld, H. R., Liesefeld, A. M., Töllner, T., & Müller, H. J. (2017). Attentional capture in visual search: Capture and post-capture dynamics revealed by EEG. *Neuroimage*, *156*, 166–173.
Lopez-Calderon, J., & Luck, S. J. (2014). ERPLAB: An open-source toolbox for the analysis of event-related potentials. *Frontiers in Human Neuroscience*, *8*, 213.
Maris, E. (2012). Statistical testing in electrophysiological studies. *Psychophysiology*, *49*, 549–565.
Maris, E., & Oostenveld, R. (2007). Nonparametric statistical testing of EEG- and MEG-data. *Journal of Neuroscience Methods*, *164*, 177–190.

Marsman, M., & Wagenmakers, E.-J. (2017). Bayesian benefits with JASP. *European Journal of Developmental Psychology*, *14*, 545–555.
Mathôt, S., Schreij, D., & Theeuwes, J. (2012). OpenSesame: An open-source, graphical experiment builder for the social sciences. *Behavior Research Methods*, *44*, 314–324.
Moher, J., & Egeth, H. E. (2012). The ignoring paradox: Cueing distractor features leads first to selection, then to inhibition of to-be-ignored items. *Attention, Perception, & Psychophysics*, *74*, 1590–1605.
Munneke, J., Van der Stigchel, S., & Theeuwes, J. (2008). Cueing the location of a distractor: An inhibitory mechanism of spatial attention? *Acta Psychologica*, *129*, 101–107.
Munoz, D. P., & Everling, S. (2004). Look away: The anti-saccade task and the voluntary control of eye movement. *Nature Reviews Neuroscience*, *5*, 218–228.
Myers, N. E., Rohenkohl, G., Wyart, V., Woolrich, M. W., Nobre, A. C., & Stokes, M. G. (2015). Testing sensory evidence against mnemonic templates. *ELife*, *4*, e09000.
Myers, N. E., Stokes, M. G., & Nobre, A. C. (2017). Prioritizing information during working memory: Beyond sustained internal attention. *Trends in Cognitive Sciences*, *21*, 449–461.
Myers, N. E., Walther, L., Wallis, G., Stokes, M. G., & Nobre, A. C. (2015). Temporal dynamics of attention during encoding versus maintenance of working memory: Complementary views from event-related potentials and alpha-band oscillations. *Journal of Cognitive Neuroscience*, *27*, 492–508.
Noonan, M. P., Adamian, N., Pike, A., Printzlau, F., Crittenden, B. M., & Stokes, M. G. (2016). Distinct mechanisms for distractor suppression and target facilitation. *Journal of Neuroscience*, *36*, 1797–1807.
Noonan, M. P., Crittenden, B. M., Jensen, O., & Stokes, M. G. (2018). Selective inhibition of distracting input. *Behavioural Brain Research*, *355*, 36–47.
Olivers, C. N., & Eimer, M. (2011). On the difference between working memory and attentional set. *Neuropsychologia*, *49*, 1553–1558.
Olivers, C. N., Meijer, F., & Theeuwes, J. (2006). Feature-based memory-driven attentional capture: Visual working memory content affects visual attention. *Journal of Experimental Psychology: Human Perception and Performance*, *32*, 1243–1265.
Olivers, C. N., Peters, J., Houtkamp, R., & Roelfsema, P. R. (2011). Different states in visual working memory: When it guides attention and when it does not. *Trends in Cognitive Sciences*, *15*, 327–334.
Onton, J., Delorme, A., & Makeig, S. (2005). Frontal midline EEG dynamics during working memory. *Neuroimage*, *27*, 341–356.
Oostenveld, R., Fries, P., Maris, E., & Schoffelen, J. M. (2011). FieldTrip: Open source software for advanced analysis of MEG, EEG, and invasive electrophysiological data. *Computational Intelligence and Neuroscience*, *2011*, 156869.
Pasternak, T., & Greenlee, M. W. (2005). Working memory in primate sensory systems. *Nature Reviews Neuroscience*, *6*, 97–107.
Payne, L., Guillory, S., & Sekuler, R. (2013). Attention-modulated alpha-band oscillations protect against intrusion of irrelevant information. *Journal of Cognitive Neuroscience*, *25*, 1463–1476.
Payne, L., & Sekuler, R. (2014). The importance of ignoring: Alpha oscillations protect selectivity. *Current Directions in Psychological Science*, *23*, 171–177.
Perrin, F., Pernier, J., Bertrand, O., & Echallier, J. F. (1989). Spherical splines for scalp potential and current density mapping. *Electroencephalography and Clinical Neurophysiology*, *72*, 184–187.
Postle, B. R. (2006). Working memory as an emergent property of the mind and brain. *Neuroscience*, *139*, 23–38.
Reeder, R. R., Olivers, C. N. L., Hanke, M., & Pollmann, S. (2018). No evidence for enhanced distractor template representation in early visual cortex. *Cortex*, *108*, 279–282.
Reeder, R. R., Olivers, C. N. L., & Pollmann, S. (2017). Cortical evidence for negative search templates. *Visual Cognition*, *25*, 278–290.
Rihs, T. A., Michel, C. M., & Thut, G. (2007). Mechanisms of selective inhibition in visual spatial attention are indexed by alpha-band EEG synchronization. *European Journal of Neuroscience*, *25*, 603–610.
Rizzolatti, G., Riggio, L., Dascola, I., & Umiltá, C. (1987). Reorienting attention across the horizontal and vertical meridians: Evidence in favor of a premotor theory of attention. *Neuropsychologia*, *25*, 31–40.
Rouder, J. N., Speckman, P. L., Sun, D., Morey, R. D., & Iverson, G. (2009). Bayesian *t* tests for accepting and rejecting the null hypothesis. *Psychonomic Bulletin & Review*, *16*, 225–237.
Ruff, C. C., & Driver, J. (2006). Attentional preparation for a lateralized visual distractor: Behavioral and fMRI evidence. *Journal of Cognitive Neuroscience*, *18*, 522–538.
Sauseng, P., Griesmayr, B., Freunberger, R., & Klimesch, W. (2010). Control mechanisms in working memory: A possible function of EEG theta oscillations. *Neuroscience & Biobehavioral Reviews*, *34*, 1015–1022.
Sauseng, P., Klimesch, W., Heise, K. F., Gruber, W. R., Holz, E., Karim, A. A., et al. (2009). Brain oscillatory substrates of visual short-term memory capacity. *Current Biology*, *19*, 1846–1852.
Sawaki, R., & Luck, S. J. (2010). Capture versus suppression of attention by salient singletons: Electrophysiological evidence for an automatic attend-to-me signal. *Attention, Perception, & Psychophysics*, *72*, 1455–1470.
Sawaki, R., & Luck, S. J. (2013). Active suppression after involuntary capture of attention. *Psychonomic Bulletin & Review*, *20*, 296–301.
Schneider, D., Göddertz, A., Haase, H., Hickey, C., & Wascher, E. (2019). Hemispheric asymmetries in EEG alpha oscillations indicate active inhibition during attentional orienting within working memory. *Behavioural Brain Research*, *359*, 38–46.
Schneider, D., Mertes, C., & Wascher, E. (2015). On the fate of non-cued mental representations in visuo-spatial working memory: Evidence by a retro-cuing paradigm. *Behavioural Brain Research*, *293*, 114–124.
Schneider, D., Mertes, C., & Wascher, E. (2016). The time course of visuo-spatial working memory updating revealed by a retro-cuing paradigm. *Scientific Reports*, *6*, 21442.
Schroeder, S. C. Y., Ball, F., & Busch, N. A. (2018). The role of alpha oscillations in distractor inhibition during memory retention. *European Journal of Neuroscience*, *48*, 2516–2526.
Serences, J. T., Ester, E. F., Vogel, E. K., & Awh, E. (2009). Stimulus-specific delay activity in human primary visual cortex. *Psychological Science*, *20*, 207–214.
Serences, J. T., Yantis, S., Culberson, A., & Awh, E. (2004). Preparatory activity in visual cortex indexes distractor suppression during covert spatial orienting. *Journal of Neurophysiology*, *92*, 3538–3545.
Silver, N. C., & Dunlap, W. P. (1987). Averaging correlation coefficients: Should Fisher's *z* transformation be used? *Journal of Applied Psychology*, *72*, 146–148.
Soto, D., Heinke, D., Humphreys, G. W., & Blanco, M. J. (2005). Early, involuntary top–down guidance of attention from working memory. *Journal of Experimental Psychology: Human Perception and Performance*, *31*, 248–261.

Soto, D., Hodsoll, J., Rotshtein, P., & Humphreys, G. W. (2008). Automatic guidance of attention from working memory. *Trends in Cognitive Sciences*, *12*, 342–348.
Spitzer, B., & Haegens, S. (2017). Beyond the status quo: A role for beta oscillations in endogenous content (re)activation. *eNeuro*, *4*, ENEURO.0170-17.2017.
Stilwell, B. T., & Vecera, S. P. (2018). Learned and cued distractor rejection for multiple features in visual search. *Attention, Perception, & Psychophysics*, *81*, 359–376.
Summerfield, C., Trittschuh, E. H., Monti, J. M., Mesulam, M.-M., & Egner, T. (2008). Neural repetition suppression reflects fulfilled perceptual expectations. *Nature Neuroscience*, *11*, 1004–1006.
Theeuwes, J. (2010). Top–down and bottom–up control of visual selection. *Acta Psychologica*, *135*, 77–99.
Tsal, Y., & Makovski, T. (2006). The attentional white bear phenomenon: The mandatory allocation of attention to expected distractor locations. *Journal of Experimental Psychology: Human Perception and Performance*, *32*, 351–363.
van Driel, J., Gunseli, E., Meeter, M., & Olivers, C. N. L. (2017). Local and interregional alpha EEG dynamics dissociate between memory for search and memory for recognition. *Neuroimage*, *149*, 114–128.
van Driel, J., Olivers, C. N. L., & Fahrenfort, J. J. (2019). High-pass filtering artifacts in multivariate classification of neural time series data. *BioRxiv*. https://doi.org/10.1101/530220.
van Driel, J., Ort, E., Fahrenfort, J. J., & Olivers, C. N. L. (2019). Beta and theta oscillations differentially support free versus forced control over multiple-target search. *Journal of Neuroscience*, *39*, 1733–1743.
van Driel, J., Swart, J. C., Egner, T., Ridderinkhof, K. R., & Cohen, M. X. (2015). (No) time for control: Frontal theta dynamics reveal the cost of temporally guided conflict anticipation. *Cognitive, Affective & Behavioral Neuroscience*, *15*, 787–807.
van Ede, F., Niklaus, M., & Nobre, A. C. (2017). Temporal expectations guide dynamic prioritization in visual working memory through attenuated α oscillations. *Journal of Neuroscience*, *37*, 437–445.
Wagenmakers, E.-J., Marsman, M., Jamil, T., Ly, A., Verhagen, J., Love, J., et al. (2018). Bayesian inference for psychology. Part I: Theoretical advantages and practical ramifications. *Psychonomic Bulletin and Review*, *25*, 35–57.
Waldhauser, G. T., Johansson, M., & Hanslmayr, S. (2012). Alpha/beta oscillations indicate inhibition of interfering visual memories. *Journal of Neuroscience*, *32*, 1953–1961.
Wang, B., & Theeuwes, J. (2018a). How to inhibit a distractor location? Statistical learning versus active, top–down suppression. *Attention, Perception, & Psychophysics*, *80*, 860–870.
Wang, B., & Theeuwes, J. (2018b). Statistical regularities modulate attentional capture. *Journal of Experimental Psychology: Human Perception and Performance*, *44*, 13–17.
Weaver, M. D., van Zoest, W., & Hickey, C. (2017). A temporal dependency account of attentional inhibition in oculomotor control. *Neuroimage*, *147*, 880–894.
Wegner, D. M., Schneider, D. J., Carter, S. R., III, & White, T. L. (1987). Paradoxical effects of thought suppression. *Journal of Personality and Social Psychology*, *53*, 5–13.
Wolfe, J. M. (1994). Guided search 2.0 a revised model of visual search. *Psychonomic Bulletin & Review*, *1*, 202–238.
Woodman, G. F., & Luck, S. J. (2007). Do the contents of visual working memory automatically influence attentional selection during visual search? *Journal of Experimental Psychology: Human Perception and Performance*, *33*, 363–377.
Worden, M. S., Foxe, J. J., Wang, N., & Simpson, G. V. (2000). Anticipatory biasing of visuospatial attention indexed by retinotopically specific alpha-band electroencephalography increases over occipital cortex. *Journal of Neuroscience*, *20*, RC63.
Zumer, J. M., Scheeringa, R., Schoffelen, J. M., Norris, D. G., & Jensen, O. (2014). Occipital alpha activity during stimulus processing gates the information flow to object-selective cortex. *PLoS Biology*, *12*, e1001965.